Clinical Anatomy of the Ultrasonography-Guided Injections for the Masticatory Muscles

Hyungkyu Bae

The Graduate School
Yonsei University
Department of Dentistry

Clinical Anatomy of the Ultrasonography-Guided Injections for the Masticatory Muscles

Directed by Professor Hee-Jin Kim, D.D.S., Ph.D.

A Doctoral Dissertation
Submitted to the Department of Dentistry
and the Graduate School of Yonsei University
in partial fulfillment of the requirements for the degree of
Doctor of Philosophy

Hyungkyu Bae

June 2022

This certifies that the Doctoral Dissertation
of Hyungkyu Bae is approved.

_____
Thesis Supervisor: [Hee-Jin Kim]

_____
[Kyung-Seok Hu: Thesis Committee Member #1]

_____
[Hand-Sung Jung: Thesis Committee Member #2]

_____
[Young-Chun Gil: Thesis Committee Member #3]

_____
[You-Jin Choi: Thesis Committee Member #4]

The Graduate School
Yonsei University
June 2022

TABLE OF CONTENTS

LIST OF FIGURES

LIST OF TABLES

Abstract

Clinical Anatomy of the Ultrasonography-Guided Injections for the Masticatory Muscles

Hyungkyu Bae

Department of Dentistry
The Graduate School, Yonsei University

(Directed by Professor Hee-Jin Kim D.D.S., Ph.D.)

The masticatory muscles have been the target structure of the minimally invasive procedure, as the subject of botulinum toxin injection for both cosmetic and clinical purposes, and as a safe space for filler injections. A sound understanding of the three-dimensional anatomy of the masticatory muscles is very important while performing various clinical procedures, including minimally invasive and surgical procedures.

Ultrasonography (US) analysis has the advantage of being able to observe the dynamic changes in anatomical structures in real-time, and to intuitively understand the adjacent structures. Therefore, it has been utilized in guided injections as well as examinations in musculoskeletal areas to visualize the adjacent structures. Anatomical understanding and guided injection through US are expected to be a novel breakthrough to perform the

minimally invasive procedures on the masticatory muscles safely. This study aimed to 1) identify the clinical anatomy of the masticatory muscles and surrounding structures through US, 2) compare the conventional blind and a novel US-guided injection techniques in a clinical trial, and 3) clarify the anatomical features of deep temporal arteries (DTAs) through ultrasonographic and cadaveric analyses, therefore proposing safe guidelines for minimally invasive procedures for the masticatory muscles.

This study has three parts, defined as follows. Part I included the identification of the anatomy of the masticatory muscles for the US-guided injection; part II included the comparison between the conventional blind injections and US-guided injections of botulinum toxin into the masseter; and Part III included identification of the clinical anatomy of the DTAs. In Part I, the temporalis, masseter, and lateral pterygoid muscle (LPM) and their surrounding structures from 160 hemifaces of 80 healthy young Korean volunteers (33 males and 47 females; mean age, 36.7 years) were analyzed using US. Since the LPM and infratemporal fossa can be observed through the space formed by zygomatic arch and mandibular notch, the location of the coronoid process (CorP), condylar process (ConP), and their midpoint (MP) were recorded and measured. In addition, the depth of the anatomical structures and LPM at the point MP were measured. In Part II, the 40 masseters from 20 healthy young Korean volunteers (10 males and 10 females with a mean age, 25.6 years) were included in the prospective clinical trial. BoNT-A (24 U) was injected into the masseter of each volunteer using the conventional blind and US-guided injection techniques on the left and right sides, respectively and

analyzed using US and three-dimensional facial scanning. In Part III, 42 adult hemifaces from 15 Korean and 6 Thai cadavers (12 males, 9 females; mean age, 79.6 years) with no history of trauma or surgical procedure on the temple area were used for anatomical study. A detailed dissection was performed to identify the locations of the anterior and posterior deep temporal arteries (ADTA and PDTA) with reference to the vertical plane passing through the zygomatic tubercle. Fifty-eight healthy young Korean participants (31 males and 27 females; mean age, 24.7 years) were included in the ultrasonographic study. The distance from the bone to the DTAs was measured at the level of the zygomatic tubercle (H_{Zt}) and the eyebrow (H_{Eb}).

In Part I, the normal anatomy of the temporalis muscle, masseter muscle, LPM, and their surrounding structures were analyzed using US. These structures were observed through the mandibular notch in all cases and located in the order from the most superficial to the deepest. The mean thicknesses of the skin and subcutaneous layer, masseter muscle, temporalis muscle, and depth of the LPM were 9.7±1.0 mm, 10.3±1.3 mm, 10.9±1.6 mm, and 30.9±1.9 mm at MP, respectively. The CorP was located 54.0±3.9 mm anterior to the tragus and 10.7±2.8 inferior to the ala-tragus line; the corresponding location for the MP and ConP were 39.6±3.3 mm and 7.8±1.6, and 25.2±3.0 mm and 4.9±1.9 mm, respectively.

In Part II, one case of paradoxical masseteric bulging was observed on the side where a conventional blind injection was performed, which disappeared after the compensational injection. The reduction in the thickness of the masseter in the resting state differed

significantly at one month after the injection between the conventional blind injection group and the US-guided injection group: by 12.4±7.6% and 18.0±9.7%, respectively [t(19)=3.059, p=0.007]. The reduction in the facial contour also differed significantly at one month after the injection between the conventional blind injection group and the US-guided injection group: by 2.0±0.7 mm and 2.2±0.8 mm, respectively [t(19)=2.908, p=0.009].

In Part III, the DTAs were not found within 7.2–12.6 mm posterior to the zygomatic tubercle; instead, the locations varied widely at the H_{Eb}. The distances between the bone and the ADTA were 1.3±0.8 mm and 1.7±1.2 mm, and those between the bone and the PDTA were 2.0±1.4 mm and 2.1±1.2 mm at H_{Zt} and H_{Eb}, respectively.

Based on the above results, this study showed the clinical anatomy and suggested the guidelines for US-guided minimally invasive procedures. A comprehensive understanding of the content will help clinicians implement safe and efficient minimally invasive procedures on the masticatory muscles.

Keywords: Ultrasonography, Minimally invasive procedure, Masticatory muscle, botulinum toxin, Filler injection, Masseter, Temporalis, Lateral pterygoid muscle

Clinical Anatomy of the Ultrasonography-Guided Injections for the Masticatory Muscles

Hyungkyu Bae

Department of Dentistry

The Graduate School, Yonsei University

(Directed by Professor Hee-Jin Kim D.D.S., Ph.D.)

I. Introduction

The demand for minimally invasive procedures has steadily and dramatically increased as the primary demand for cosmetic surgery shifted from surgery to minimally invasive

procedures The number of minimally invasive procedures increased by 174% in 2020 compared to 2000, of which botulinum toxin type A injection and soft tissue filler injections accounted for 33% and 26% of the total cases, respectively (Statistics, P.S.P., 2021). As the demand has increased, various complications of minimally invasive facial procedures have been reported, from bruises and pain to blindness and death in the worst cases (Levi et al., 2012; Beleznay et al., 2015). In order to avoid these complications, a sound anatomical understanding of the target area is required.

The masticatory muscle consists of four major muscles that are innervated by the motor branch of the mandibular nerve of the trigeminal nerve: the masseter, temporalis, and the medial and lateral pterygoid muscles. These muscles work in harmony with each other to perform physiological functions, such as chewing, speaking, and swallowing, by controlling the movements of the mandible (Horio et al., 1989; Isola et al., 2018). The masticatory muscles have been the target structure of the minimally invasive procedure, as the site for botulinum toxin injection for both cosmetic and clinical purposes, and are considered a safe region for filler injections. The detailed indications are as follows.

Botulinum toxin injection into the masseter muscle

The application of botulinum toxin in the facial area first began in the 1970s by being injected into the extraocular muscles to treat strabismus, and Moore and Wood expanded its use in 1994 as a treatment for masseter hypertrophy. (Guyuron et al., 1994; Moore et al., 1994; To et al., 2001; Wu, 2010). Botulinum toxin injections into the masseter muscle are becoming increasingly popular, particularly among Asian cultures, where the oval facial form and slender lower face are considered ideal (Wu, 2010; Ahn et al., 2004; Cheng et al., 2019). These injections are utilized not only to minimize masseter hypertrophy for aesthetic reasons, but also for therapeutic purposes to treat bruxism and clenching (Ahn et al., 2004; Lee et al., 2010). Botulinum toxin injection is considered to be an ideal procedure due to its dramatic effect, less side effects than invasive surgeries, and reversibility of the results when the appropriate dose is administered (Garcia et al., 1996).

Paradoxical masseteric bulging (PMB) is one of the most frequent sequelae of botulinum toxin injection into the masseter. Lee et al. (2016) reported the occurrence of PMB after injecting botulinum toxin into the masseter, while Kim et al. (2005) reported that uneven bulging of muscles on the facial surface occurred 2 to 4 weeks after injections, especially in male patients with thin facial skin (Lee et al., 2016; Kim et al., 2005). The incidence of PMB varies greatly in the literature and is reported from 0.15% to 27.3%

(yeh et al., 2018). Currently, the most common approach is to inject botulinum toxin deeply into the lower third of the masseter, in order to avoid diffusion or unintended injection into surrounding tissues including the facial expression muscles and parotid gland (Kim et al., 2016). Lee et al. (2016) suggested that the deep inferior tendon (DIT) located inside the muscle may cause PMB by preventing the spread of toxin in the deep injection method (Lee et al., 2016). However, it is nearly impossible to determine the internal location of the DIT with the naked eye or by palpating, which represents a limitation of blind injections based on the presence of the DIT.

Botulinum toxin injection into the lateral pterygoid muscle

The lateral pterygoid muscle (LPM) is the masticatory muscle located within the infratemporal fossa, and functions as a protrusion, depression, and unilateral movements of the mandible. This muscle consists of the upper and lower head, which originates from the sphenoid bone and inserts into the mandible (Murray et al., 2004; Murray et al., 2007). Some anatomical and histological studies revealed that some fibers of the LPM are continuously attached to the articular disc and fibrous capsule of the temporomandibular joint (Heylings et al., 1995; Fujita et al., 2001; Peterson et al., 1996). As this muscle is involved in functional movements of the mandible and is directly connected to the temporomandibular joint, the relation between the temporomandibular disorder (TMD)

and this muscle has been steadily suggested (Juniper, 1984; Fujita et al., 2001; Wongwatana et al., 1994).

Numerous studies reported TMD management by injecting botulinum toxin into the LPM. Since the LPM is located deep in the infratemporal fossa and is covered by other major anatomical structures, including masseter muscle and mandibular ramus, the accuracy of the traditional approach of blind injection is questionable. Therefore, a method of approaching the LPM under the guidance of computed tomography (CT) or magnetic resonance imaging (MRI) has been proposed (Yoshida, 2018; Pons et al., 2019). This enables accurate injections; however, the procedure is complex and requires more time and cost. Few studies have suggested the possibility of accessing the infratemporal fossa and LPM through the mandibular notch (or sigmoid notch) under US guidance (Chen et al., 2018; Anugerah et al., 2020; Qin et al., 2020). US visualize the anatomical structures in real-time and allow their quantitative measurement, making it suitable for locating deeply positioned LPM. Moreover, the process is relatively simple and has advantages in terms of time and cost. However, since the space, consisting of a zygomatic arch and a mandibular notch, is small and difficult to locate, an approach protocol needs to be established. In addition, locating and analyzing the LPM and its surrounding structures under US guidance has not yet been well studied.

Temple augmentation using filler injections

The depression of the temple area significantly contributes to an aged appearance in the frontal and lateral views and can be exaggerated by skin atrophy and depletion of fat and muscles. Therefore, filler injections are commonly administered in this area to compensate for temporal depression. These injections provide a more youthful appearance with minimal or no scarring, little bleeding, no hair loss, and no requirement to undergo major surgery (Raspaldo, 2012a).

Physicians should always consider the multilayered contents of the temporal fossa and interlaced vascular structures while performing temple augmentation procedures. Anastomosed blood vessels are abundantly distributed over the layers of the facial and temporal regions (Nakajima et al., 1995; Pinar et al., 2006; Quisling et al., 1975). Therefore, injection of fillers into the arteries that are distributed in the temporal region, including the superficial temporal artery (STA) and deep temporal arteries (DTA), may cause serious complications, such as blindness and cerebral infarction (Thanasarnaksorn et al., 2018). The supraperiosteal plane is considered to be a safe injection site because major blood vessels (such as the STA and middle temporal vein) run superficially to this plane (Beleznay et al., 2015; Jung et al., 2014a; Kim et al., 2016). However, DTAs are known to run between the temporalis muscles and bone surface in the temporal fossa; there is a risk of the injection being inserted supraperiosteally (Standring et al., 2005).

DTAs are branches of the second part of the maxillary artery, which pass through the supraperiosteal layer of the temporal fossa. DTAs may also anastomose with other nearby arteries, including the lacrimal, supraorbital, and middle meningeal arteries (Amans et al., 2014; Quisling and Seeger, 1975). This suggests the risk of blindness involving these anastomotic connections when intra-arterial injection is administered during temple augmentation. Some studies reported cases of blindness caused by temple augmentation (Chen et al., 2014). Despite their clinical importance, there are only a few reports on the precise clinical anatomy of DTAs (Nakajima et al., 1995).

US observe dynamic changes in the anatomical structures in real-time and intuitively understand the adjacent structures. In addition, the Doppler mode of US can identify the location and type of blood vessels by analyzing the location and speed of blood flow within the soft tissue. US can easily analyze the z-axis data (or depth data) of the anatomical structures, which was relatively limited in the traditional dissection analysis.

US guidance has recently been utilized to administer injections and to examine the musculoskeletal areas (Ciftci et. al., 2013; von Coelln et al., 2008; Church et. Al, 2017; Ruiz Santiago et al., 2019). Since the target structure or space and needle position can be identified in real-time, US is used when targeting small muscles or precisely injecting them at a specific position. The ability to visualize anatomical variations provides safety and reliability during US-guided injections.

As described previously, there are some challenges in performing minimally invasive procedures for masticatory muscles in the facial area. Anatomical understanding and the guided injection through US are expected to be novel breakthroughs in solving these problems. Therefore, our study aimed to 1) identify the clinical anatomy of the masticatory muscles and surrounding structures under US guidance, 2) compare the conventional blind and a novel US-guided injection techniques in a clinical trial, 3) clarify the anatomical features of DTAs through ultrasonographic and cadaveric analyses, and thereby proposing safe guidelines for minimally invasive procedures for the masticatory muscles.

II. Materials and Methods

Part I: Normal US anatomy of the masticatory muscles for the US-guided injection

Subjects

The study was conducted in accordance with the guidelines of the Declaration of Helsinki and was approved by the Institutional Review Board of Yonsei University Dental Hospital (IRB no. 2-2017-0023).

This study included 160 hemifaces from 80 healthy young Korean volunteers (33 males and 47 females; age, 36.7±3.5 years [mean±SD]). The exclusion criteria were as follows: patients with (1) temporomandibular joint disorder; (2) obvious facial asymmetry; (3) history of plastic surgery; and (4) history of receiving a botulinum toxin injection within the preceding six months.

Before in the ultrasonographic study, each volunteer provided a signed written consent form. The potential side effects were fully explained to the participants, and they were free to withdraw from the study at any time. The exclusion criteria for this study included pregnancy, a history of drug allergy, any serious medical illnesses, or surgical or nonsurgical treatment in the facial area within the preceding six months.

US analysis protocol

A real-time two-dimensional B-mode US device with a high-frequency (15 MHz) linear transducer (E-CUBE 15 PLATINUM, ALPINION, Seoul, Korea) was used to obtain ultrasonographic images. All the landmarks and reference lines were drawn on the skin using waterproof eyeliner prior to US analysis. The ultrasound gel (SONO JELLY, MEDITOP Corporation, Youngjin, Korea) was thickly applied to the skin surface. At each reference point and line, the transducer was positioned so that the left side of the image indicated the direction of the medial or superior. US images were obtained with the volunteer in the upright seated position. After the US procedure, cleaners and moisturizers were provided for patient convenience.

Normal US anatomy of the temporalis muscle

The following reference lines were designated for the US analyses of the temporalis muscle (Figure 1): (1) the vertical plane passing through the zygomatic tubercle perpendicular to the zygomatic arch (VP), (2) the horizontal line passing through the zygomatic arch (H_{Za}), (3) the horizontal line passing through the zygomatic tubercle parallel to H_{Za} (H_{Zt}), and (4) the horizontal line passing through the eyebrow parallel to H_{Za} (H_{Eb}). US images were taken at two horizontal planes: H_{Zt} and H_{Eb}.

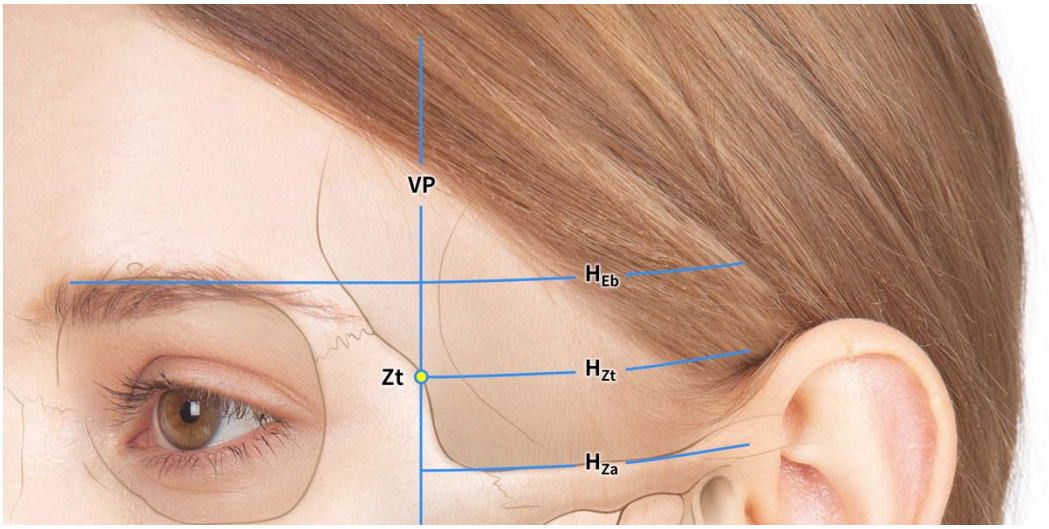

Figure 1. Reference lines for dissections, measurements, and ultrasonographic analyses

Zt., zygomatic tubercle; VP, the vertical plane passing through the zygomatic tubercle perpendicular to the zygomatic arch; H_{Za}, the horizontal line passing through the zygomatic arch; H_{Zt}, the horizontal line passing through the zygomatic tubercle parallel to H_{Za}; H_{Eb}, the horizontal line passing through the eyebrow level parallel to H_{Za}

Normal US anatomy of the masseter muscle

The following reference lines were designated for the US analyses of the masseter muscle (Figure 2): (1) the line passing through the cheilion and otobasion inferius (designated as T1), (2) the line corresponding to the lower margin of the mandible (designated as T3), (3) the line located between T1 and T3 (designated as T2), and (4) the lines trisecting the masseter longitudinally (designated as L1 and L2). All of these reference lines were drawn on the skin with waterproof eyeliner prior to performing the injections and measurements. US images were taken at three horizontal and two vertical planes: T1, T2, T3, L1, and L2.

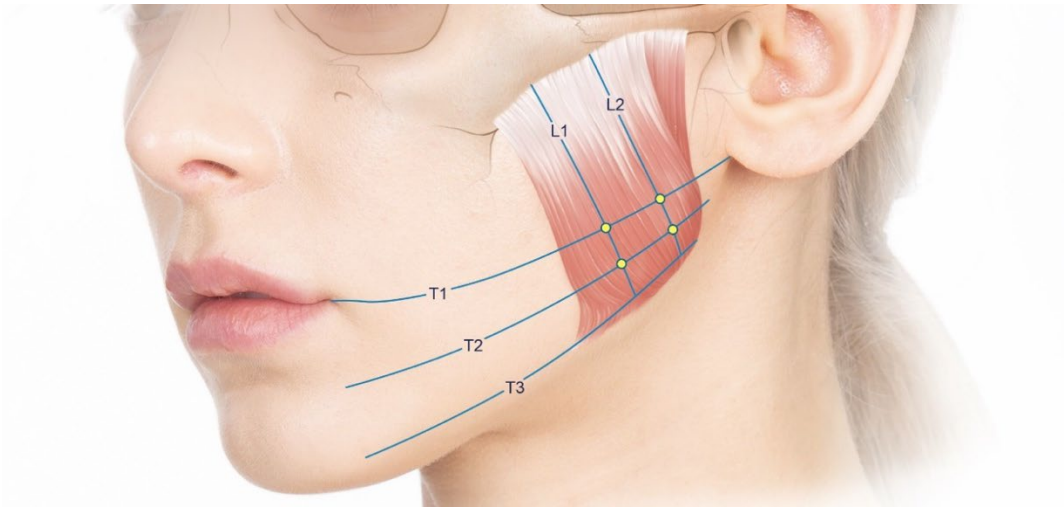

Figure 2. Reference lines for the injections and measurements

T1, the line passing through the cheilion and otobasion inferius; T2, the line located between T1 and T3; T3, the line corresponding to the lower margin of the mandible; L1 and L2, the lines trisecting the masseter muscle longitudinally

Normal US anatomy of the LPM

US analysis was performed with the patient's mouth open 2 cm to facilitate access to the LPM through the mandibular notch. The transducer was initially positioned perpendicular to the skin. Then, the transducer was aligned and rotated to find the location where the coronoid and condylar processes were simultaneously observed on the same plane. The US image was taken at this location, the location of the transducer was recorded, and the photograph of the side view of the volunteer was taken. Based on the locations of the coronoid process and condylar process on the US image and the location of the transducer in the side view photograph, the following reference points were defined, and their positions were measured with reference to the ala-tragus line (Figure 3A): (1) location of the coronoid process (designated as CorP), (2) location of the condylar process (designated as ConP), and (3) the midpoint between CorP and ConP (designated as MP). The thickness of the skin and subcutaneous layer, masseter muscle, and temporalis muscle, and the distance from the skin to the LPM at the MP were measured using the ImageJ program (Figure 3B, C) (National Institutes of Health, Bethesda, MD, USA).

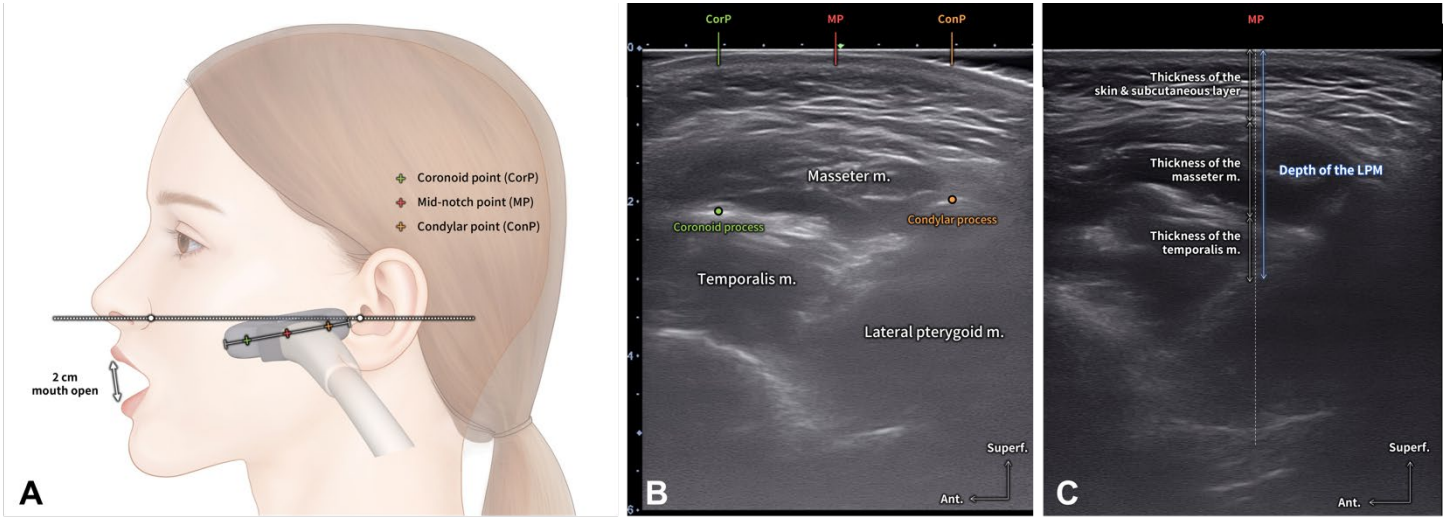

Figure 3. Ultrasonographic imaging and measurement protocol of lateral pterygoid muscle (LPM)

(A) The location where the coronoid process and the condylar process were simultaneously observed at the same plane (B) Ultrasonography of the LPM and infratemporal fossa (B mode, 15-MHz linear transducer) (C) Measurement of the thickness of the skin and subcutaneous layer, the thickness of the masseter muscle, and the temporalis muscle, and the distance from the skin to the LPM at the point MP

Part II: Comparison between the conventional blind injections and US-guided injections of botulinum toxin into the masseter

Subjects

Forty masseters from 20 healthy young Korean volunteers (10 males and 10 females with a mean age, 25.6 years) were included in this prospective clinical trial. All of the volunteers had the complaint of a bulky masseter, and four of them had a myofascial masseteric pain. Before participating in the study, a signed written consent form was obtained from each volunteer. Each volunteer was a dental student or staff member at the College of Dentistry, Yonsei University, Seoul, Korea. Potential side effects were fully explained to the subjects, and they were free to withdraw from the treatment and research at any time. The exclusion criteria for this study included pregnancy, a history of drug allergy, any other serious medical illnesses, or surgical or nonsurgical treatment in the facial area (including botulinum toxin injection) in the previous six months. All the study procedures were approved by the institutional review board of the Yonsei University College of Dentistry (IRB No. 2-2019-0008).

Injection method

Twenty-four units of BoNT-A (Innotox, 1.25 mL/vial, 4 units/0.1 mL; Medytox Inc., Seoul, South Korea) were injected into the masseter of each volunteer using the conventional blind and US-guided injection techniques on the left and right sides, respectively. The injection locations for the masseter were determined in accordance with the conventional blind injection guideline. Botulinum toxin was injected at four crossing points of the aforementioned reference lines (T1 and L1, T1 and L2, T2 and L1, and T2 and L2) for each masseter. To avoid producing an iatrogenic tattoo with the marking ink, the actual injection was administered adjacent to the indicated injection location. The site of maximal protrusion during clenching was included among the four injection locations.

A conventional injection was administered on the left side masseter of each volunteer using an 8-mm-long 30-G BD syringe, which is widely used in clinical practice. The needle was inserted perpendicularly at each injection location. The needle tip was inserted until it pressed lightly against the bone, and then 6 U of botulinum toxin was injected (Figure 4A).

A US-guided injection was administered on the right side masseter of each volunteer using a 25-mm-long 30-G needle to cover the whole masseter without applying any pressure. After confirming the locations of the masseter, internal DIT, and surrounding structures using a US device, a US-guided injection was administered using an out-of-plane technique with the transducer located along T1 and T2 (Figure 4B). The injection

locations were the same as that in the conventional blind injection; however, botulinum toxin was injected into parts that were both deeper and more superficial than the DIT (Figure 5). Moreover, along with the perpendicular movement of the needle tip at each injection site, backward and forward movements were also performed to administer injections precisely according to the shape and DIT type of the masseter under US guidance. The dose of the toxin was divided based on the thicknesses of the superficial and deep parts. The total dose (24 U) of the US-guided injections was the same as that of the conventional blind injections. All the injections were administered by the same person. Each volunteer was examined using a three-dimensional (3D) facial scanning and US imaging before and after the injection. Volunteers were guided to contact the researchers immediately if there were any side effects or discomfort, such as PMB. The volunteers were followed up one month after the injection when they revisited for a US imaging and facial scanning.

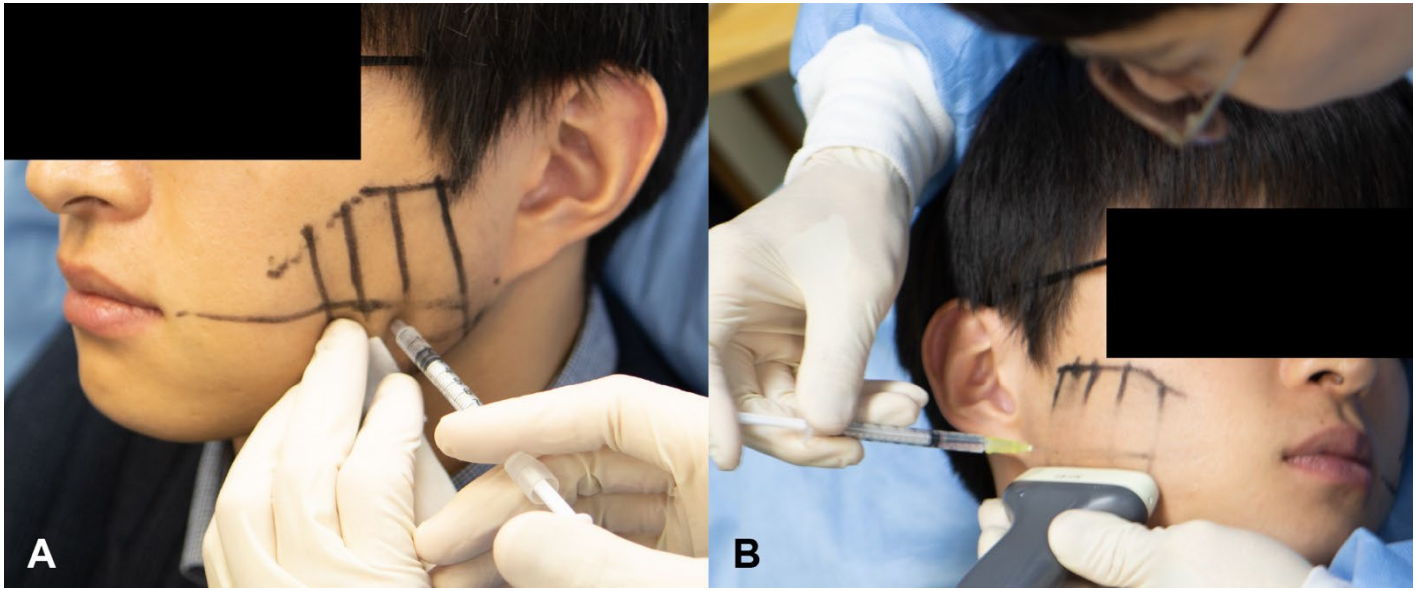

Figure 4. Injecting 24 U of botulinum toxin

(A) Using the conventional blind injection method on the left side and (B) Using the US-guided injection method on the right side

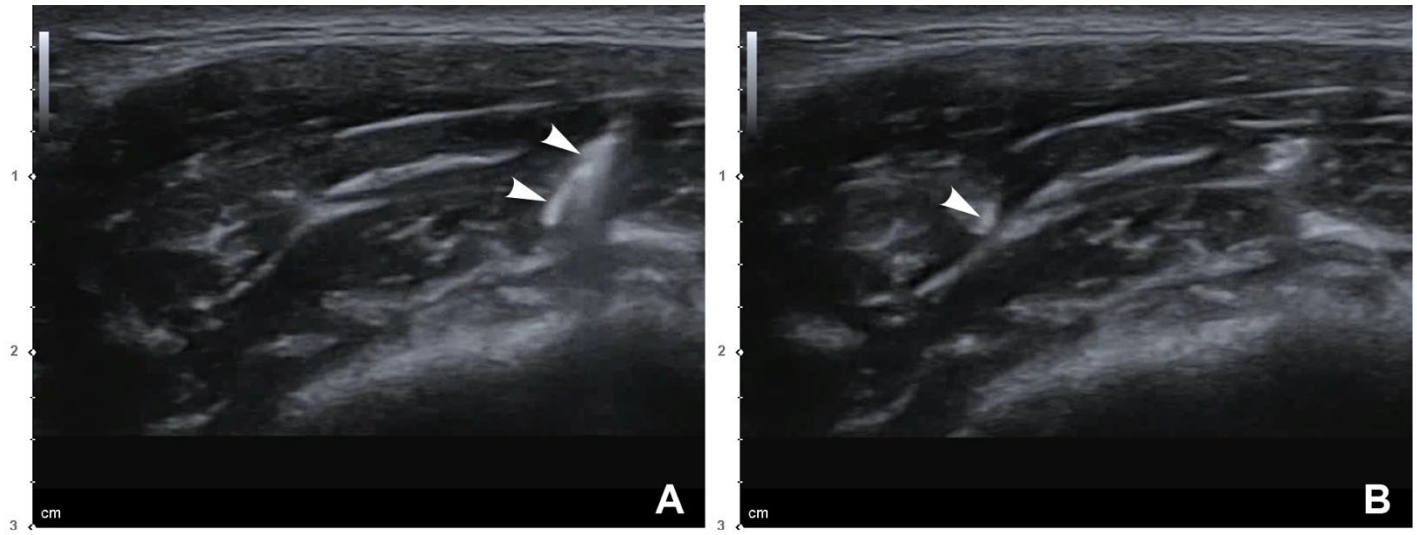

Figure 5. Ultrasonography-guided dual-plane botulinum toxin injections into the masseter

White arrowheads indicate a needle tip: (A) Deep injection (B mode, transverse view, 15-MHz linear transducer) and (B) Superficial injection (B mode, transverse view, 15-MHz linear transducer)

US-based analysis of the thickness of the masseter

The patients were placed in a semi-supine position for the US examination and injection. US images of the masseters on 40 sides were obtained using a real-time two-dimensional B-mode US device with a high-frequency (15 MHz) linear transducer (E-CUBE 15 PLATINUM, ALPINION MEDICAL SYSTEMS Co., Ltd., Seoul, Korea).

After applying a US gel thickly, the transducer was positioned just above the skin surface at each reference line. Special efforts were made to avoid mechanical pressure from the US probe distorting the soft tissue. Each US video was taken before and one month after the injection in both resting and clenching states.

A US image was taken with the probe placed horizontally on the T1 line (Figure 6). Starting in the most-relaxed state, the process of clenching and relaxing was repeated twice, and corresponding images were taken. The muscle thickness was assessed by measuring the thickest part of the muscle perpendicular to the mandibular ramus. All the measurements were taken by an investigator who did not administer the injection, and the investigator was unaware of the methods and the sites of injection.

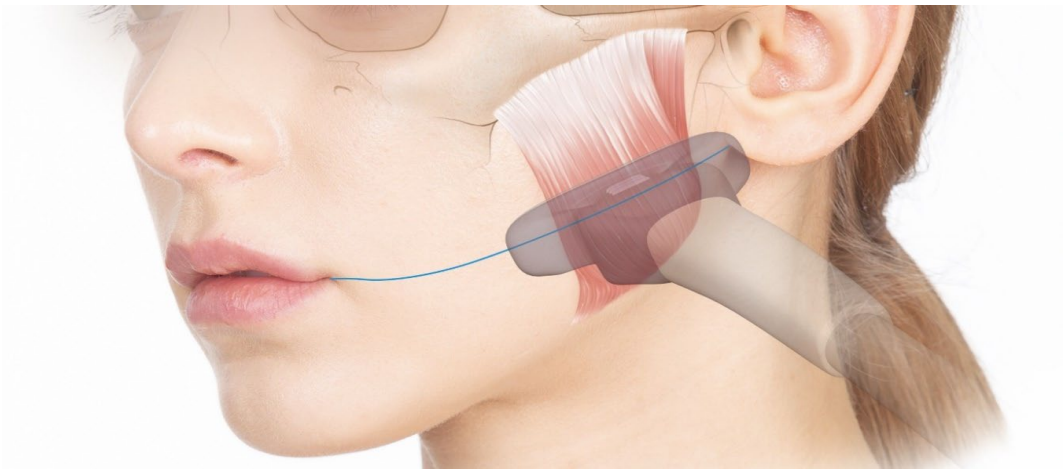

Figure 6. Reference location of transducer for masseter thickness measurement

The transducer was applied over the T1 line to obtain a ultrasonographic video of the masseter during the process of clenching and relaxing again, starting in the relaxed state.

T1, the line passing through the cheilion and otobasion inferius

Three-dimensional analysis of the facial contour before and after the injection

The volunteers' faces were scanned before and one month after the injection using a structured-light scanner (Morpheus 3D®, Morpheus Co. Ltd., Seongnam, Korea). One frontal view and two oblique views were first scanned and then merged through a geometry analysis of the nearby areas at three locations (lateral canthus, alare, and cheilion) bilaterally. A 3D model was obtained using the Morpheus Plastic Solution (version 3.0) software (MPS 3.0; Morpheus Co. Ltd.).

The scanned images were superimposed using the MPS 3.0 program. The depth difference between the scanned face before and one month after the injection was automatically measured in the direction perpendicular to the facial surface and is displayed in different colors (Figure 7). The location with the largest depth difference in each volunteer was measured and analyzed. Similar to that of the US-based analysis, all measurements were made by an investigator who did not administer the injection and was unaware of the injection methods and sites.

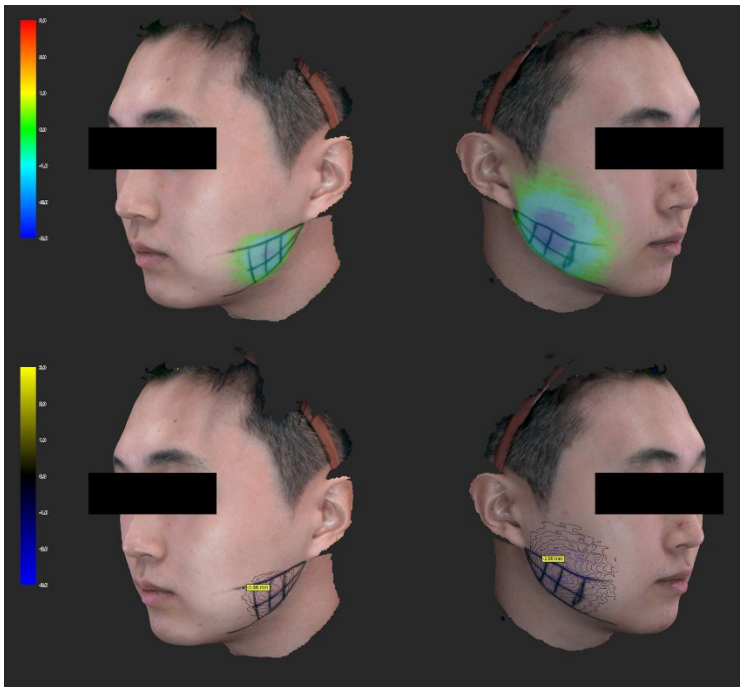

Figure 7. 3D scanned model of the facial changes in a volunteer

The amount of facial contour change is expressed in both colors and values. The location with the largest difference in each volunteer was measured and analyzed.

Statistical analyses

The contour changes in the face measured by 3D scanning and the changes in the masseter thickness measured by US were analyzed using a paired t-test after the Kolmogorov-Smirnov test had been applied to check for normality. The probability criterion for statistical significance was $p<0.05$. The statistical analysis was performed using SPSS software (version 23.0 for Windows, SPSS, Chicago, IL, USA).

Part III: Clinical anatomy of the DTAs

Topographic location of the DTAs

The cadavers used in the present study were legally donated to the institutes and subjected to dissection of the temple area after receiving approval from the Surgical Anatomy Education Center, Yonsei University College of Medicine. The subjects had provided consent for donating their bodies for research purposes.

Forty-two hemifaces from 15 Korean and six Thai cadavers (12 males, 9 females; mean age, 79.6 years) were dissected in this study. All cadavers had been donated legally to the Yonsei Medical Center (Seoul, Republic of Korea) and Chulalongkorn University (Bangkok, Thailand) and had no history of trauma, neuromuscular disorder, or surgical procedures in the temple area. To enable clear observations of the arterial branches of the face, latex (Neoprene, Lot No. 307L146, DuPont, Barsac, France) was injected into all specimens through the common carotid artery prior to dissection. The skin and subcutaneous tissues of the specimens were carefully removed to expose the temporalis muscle. A detailed dissection was performed to expose and preserve the anterior deep temporal artery (ADTA) and the posterior deep temporal artery (PDTA). The overlying temporalis muscles were carefully cut and retracted to expose the underlying vascular structures.

After meticulous dissection, the locations of the DTAs were measured and analyzed with reference to the VP at the H_{Za}, H_{Zt}, and H_{Eb} levels. At each level, the distances between the VP and DTAs were measured using the ImageJ software (National Institutes of Health, Bethesda, MD, USA). If a DTA had several branches, the location of each branch was measured separately.

Depth of the DTAs

A real-time two-dimensional US device (NextGen LOGIQ E, GE Healthcare, Seoul, Korea) equipped with a high-frequency (8–18 MHz) linear transducer (L8-18I-RS) was used to obtain US Doppler mode images. All the aforementioned landmarks and reference lines were drawn on the skin using waterproof eyeliner prior to performing the injections and measurements. The US images were obtained at two reference lines, H_{Zt} and H_{Eb}. US images of the temporalis muscle and its adjacent anatomical structures were obtained by placing a transducer horizontally on each reference line. All participants were in an upright sitting position, and the transducer was positioned perpendicular to the skin surface at each reference line using a thick layer of US gel. The DTAs were located using the Doppler mode, and the pulse was checked to confirm that the vessels were arteries. Special efforts were made to avoid mechanical pressure from the transducer, which would distort the soft tissue. After obtaining the images, the distance between the bone and the DTAs was measured using the ImageJ software (Figure 8, 9).

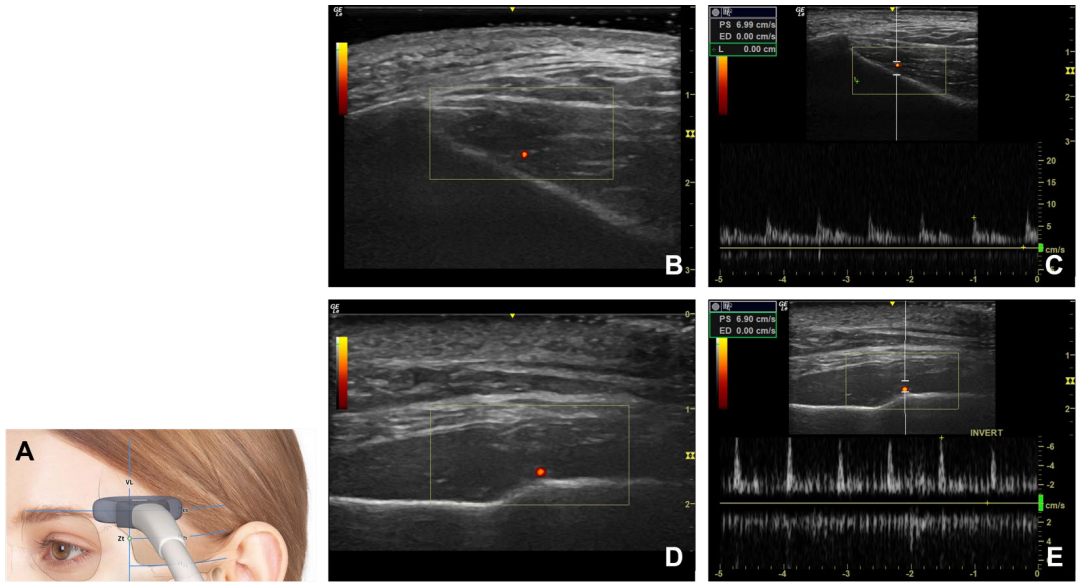

Figure 8. Ultrasonographic analysis of the deep temporal arteries at the level of H_{Eb} (15 MHz by a linear transducer)

(A) Illustration representing ultrasonographic analysis at the level of H_{Eb} (B) Doppler mode image of the anterior deep temporal artery (ADTA) at the level of H_{Eb} (C) Spectral Doppler mode image of the ADTA at the level of H_{Eb} (D) Doppler mode image of the posterior deep temporal artery (PDTA) at the level of H_{Eb} (E) Spectral Doppler mode image of the PDTA at the level of H_{Eb}

H_{Eb}, the horizontal line passing through the eyebrow parallel to the zygomatic arch

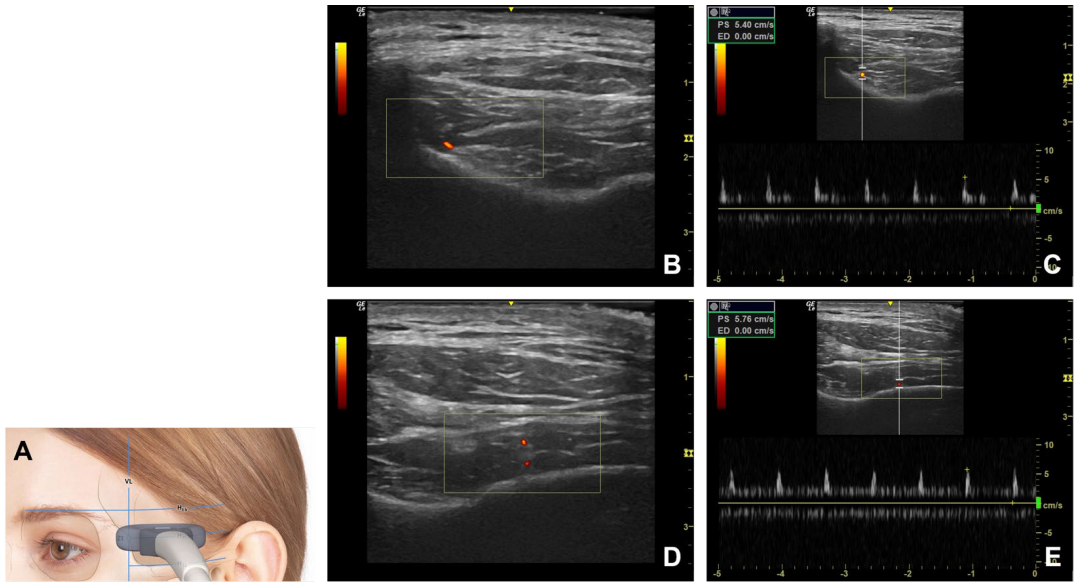

Figure 9. Ultrasonographic analysis of the deep temporal arteries at the level of H_{Zt} (15 MHz by a linear transducer)

(A) Illustration representing ultrasonographic analysis at the level of H_{Zt} (B) Doppler mode image of the anterior deep temporal artery (ADTA) at the level of H_{Zt} (C) Spectral Doppler mode image of the ADTA at the level of H_{Zt} (D) Doppler mode image of the posterior deep temporal artery (PDTA) at the level of H_{Zt} (E) Spectral Doppler mode image of the PDTA at the level of H_{Zt}

H_{Zt}, the horizontal line passing through the zygomatic tubercle parallel to the zygomatic arch

III. Results

Part I: Normal US anatomy of the masticatory muscles

Normal US anatomy of the temporalis muscle area

Line H_{Eb}

H_{Eb} is the horizontal line passing through the eyebrow parallel to H_{Za}. Since the eyebrow and hair are located at the corresponding level, these structures can be observed on the skin surface in US images. The multilayered structure of the temple area is observed in the US image. The epidermis and dermis are shown as thin hyperechoic lines, while the thin subcutaneous layer is shown as an irregular hypoechoic layer. Superficial temporal fascia (STF) is shown as a hyperechoic line, and a hypoechoic frontalis muscle may appear continuously with this layer in the anterior aspect. A thin sub-superficial musculoaponeurotic system (SMAS) layer composed of adipose tissue is observed as hypoechoic layer directly under the STF. A deep temporal fascia (DTF) is observed as one or two strong hyperechoic bands, and a temporal fat pad is observed as a hypoechoic line between the two layers. At this location, the temporalis muscle is observed as a thin hypoechoic layer and is located directly above the bony surface of the temporal fossa (Figure 10).

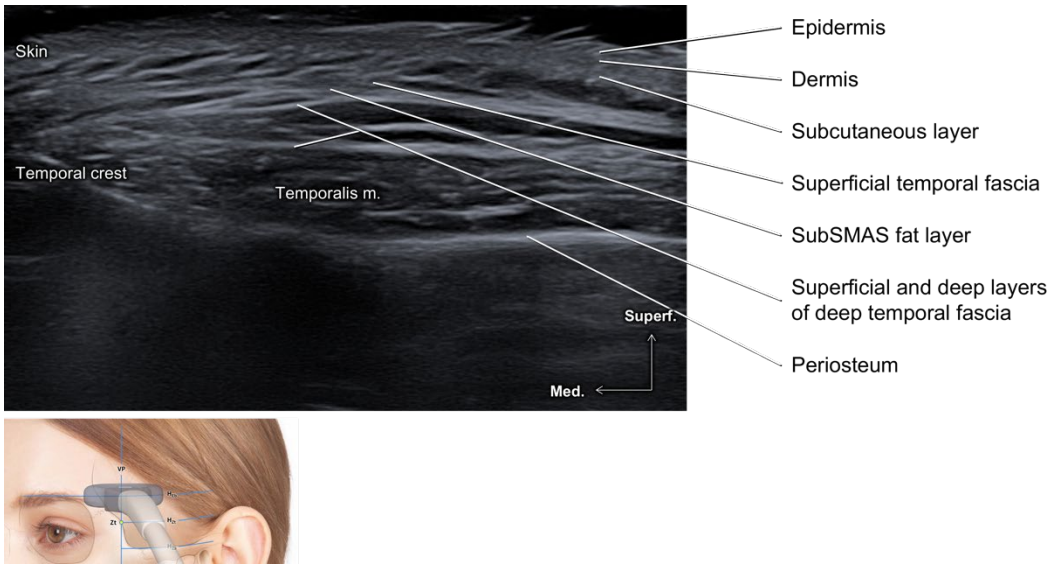

Figure 10. Ultrasonography of the transverse line passing the eyebrow (H_{Eb}), B mode (transverse view, 15 MHz by linear transducer)

SMAS, superficial musculoaponeurotic system

Line H_{Zt}

H_{Zt} is the horizontal line passing through the zygomatic tubercle parallel to H_{Za}. The zygomatic tubercle protrudes from the area where the frontal and zygomatic bones are sutured. The anterior part of the temporal fossa is obscured by the zygomatic tubercle and is not observed in the US image. Since the skin and the surface of the temporal fossa are not parallel, the surface of the temporal fossa is observed as a blurred line on the US image.

The US image at this position is similar to that of H_{Eb}; however, it differs in the following aspects: In the medial aspect, the orbicularis oculi muscle is observed on the same layer as the STF. DTF is clearly divided into deep and superficial layers, and the temporal fat pad is clearly observed between them. Immediately below the DTF, a temporal extension of the buccal fat pad is observed as a slightly hyperechoic area (Figure 11).

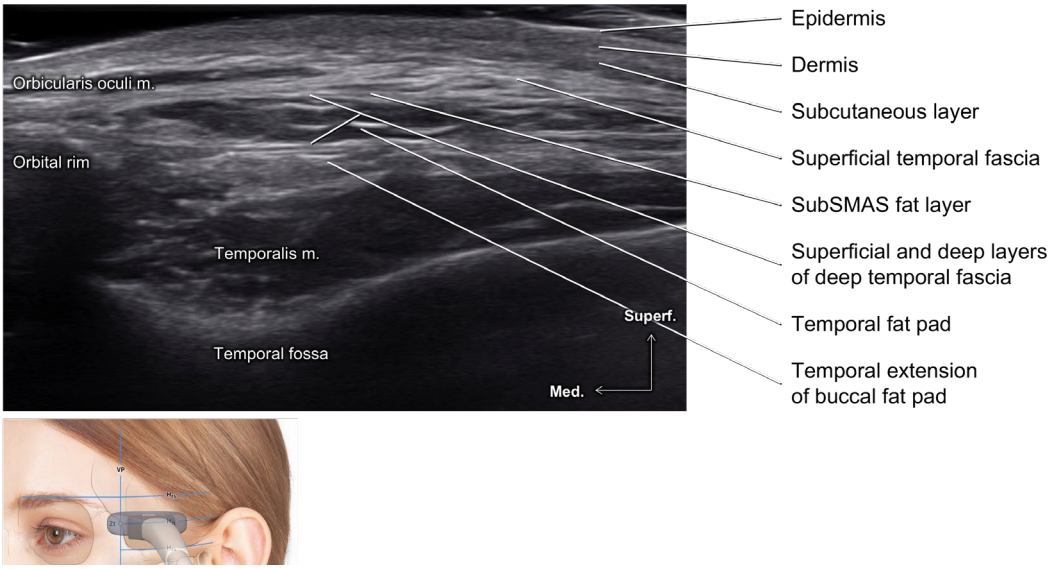

Figure 11. Ultrasonography of the transverse line passing the zygomatic tubercle (H_{Zt}), B mode (transverse view, 15 MHz by linear transducer)

SMAS, superficial musculoaponeurotic system

Normal US anatomy of the masseter muscle area

Line T1

T1 is the line passing through the cheilion and otobasion inferius. At this location, the epidermis, dermis, and subcutaneous layers appear typically. The surface of the mandibular ramus is observed as a strong hyperechoic line in the deepest location. The cross-section of the masseter muscle is observed as hypoechoic and ovoid areas. Inside the masseter muscle, several DITs are observed as hyperechoic lines. The uniformly hyperechoic parotid gland is located posterior to the masseter muscle, and the platysma muscle is observed as a hypoechoic line on the surface of the masseter muscle and parotid gland. A hypoechoic extension of the buccal fat pad is observed anterior to the masseter muscle (Figure 12).

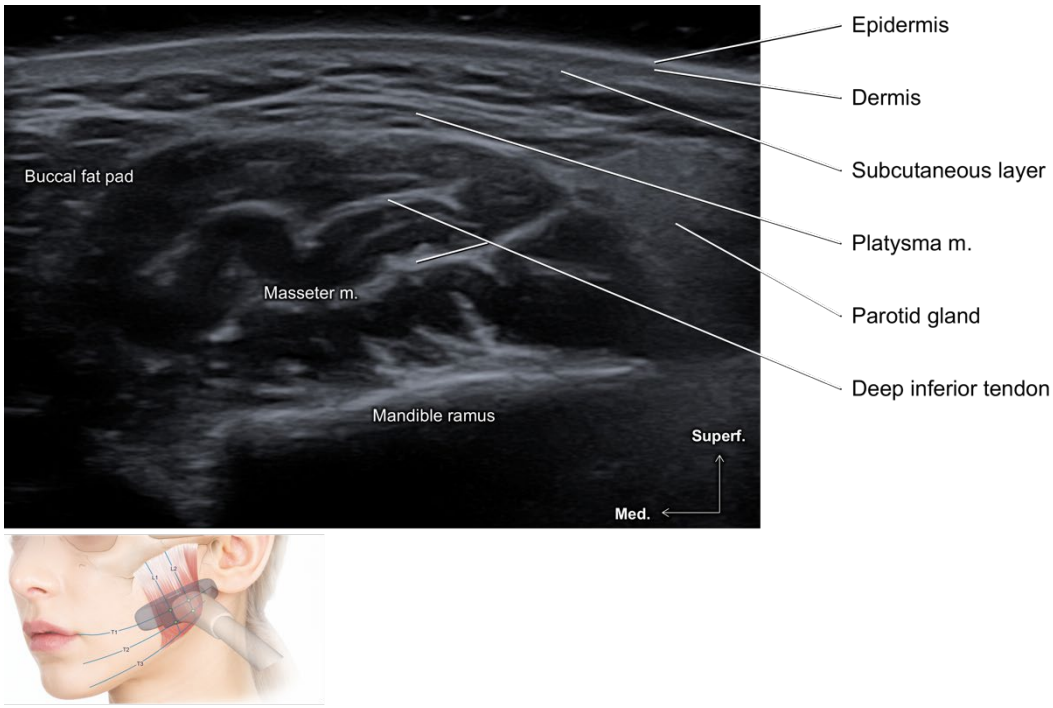

Figure 12. Ultrasonography of the transverse line passing the cheilion and otobasion inferius (T1), B mode (transverse view, 15 MHz by linear transducer)

Line T2

T2 is the line located between T1 and T3. Similar to that in T1, thin hypoechoic platysma muscle covering the masseter muscle and a strong hyperechoic parotideomasseteric fascia are also observable in the T2 area. At this location, DIT is clearly observable and divides the masseter muscle into deep and superficial layer (Figure 13).

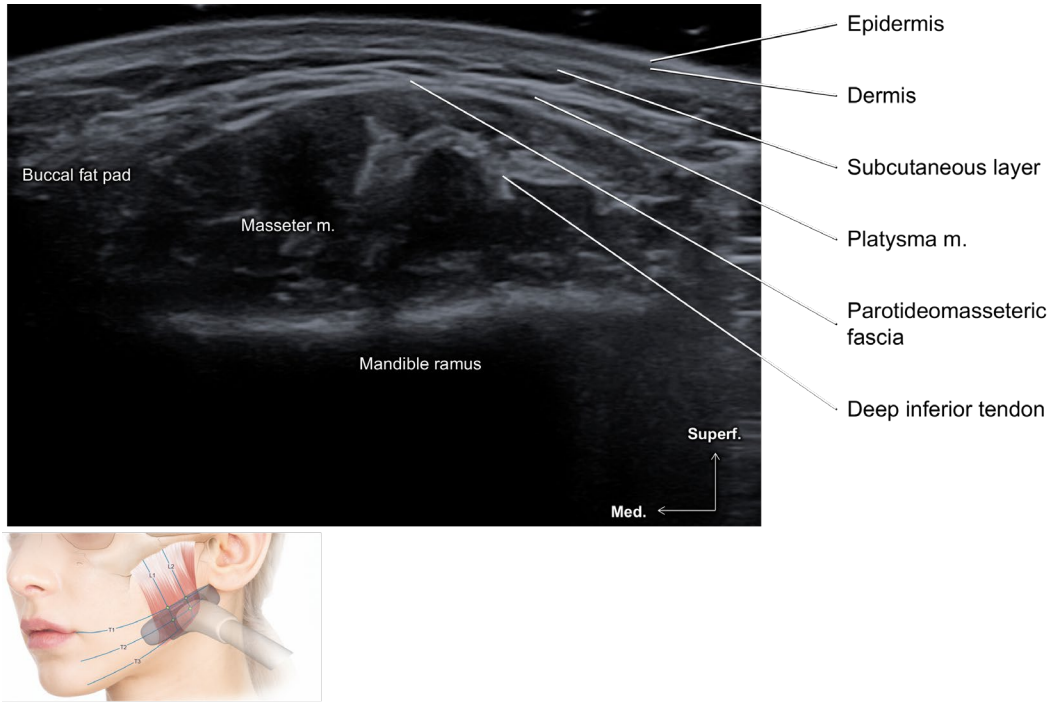

Figure 13. Ultrasonography of the transverse line located between T1 and T3 (T2) B mode, (transverse view, 15 MHz by linear transducer)

T1, the transverse line passing the cheilion and otobasion inferius; T3, the transverse line corresponding to the lower margin of the mandible

Line T3

T3 is the line corresponding to the lower margin of the mandible. In T3, the masseter muscle is observed as thinner compared to that in T1 and T2. A thin hypoechoic platysma muscle and a strong hyperechoic parotideomasseteric fascia surrounding the masseter muscle and parotid gland are observable. Facial vessels are observed as an anechoic circular space anterior to the masseter muscle. As they are thick blood vessels, their shape is well observed in B mode (Figure 14).

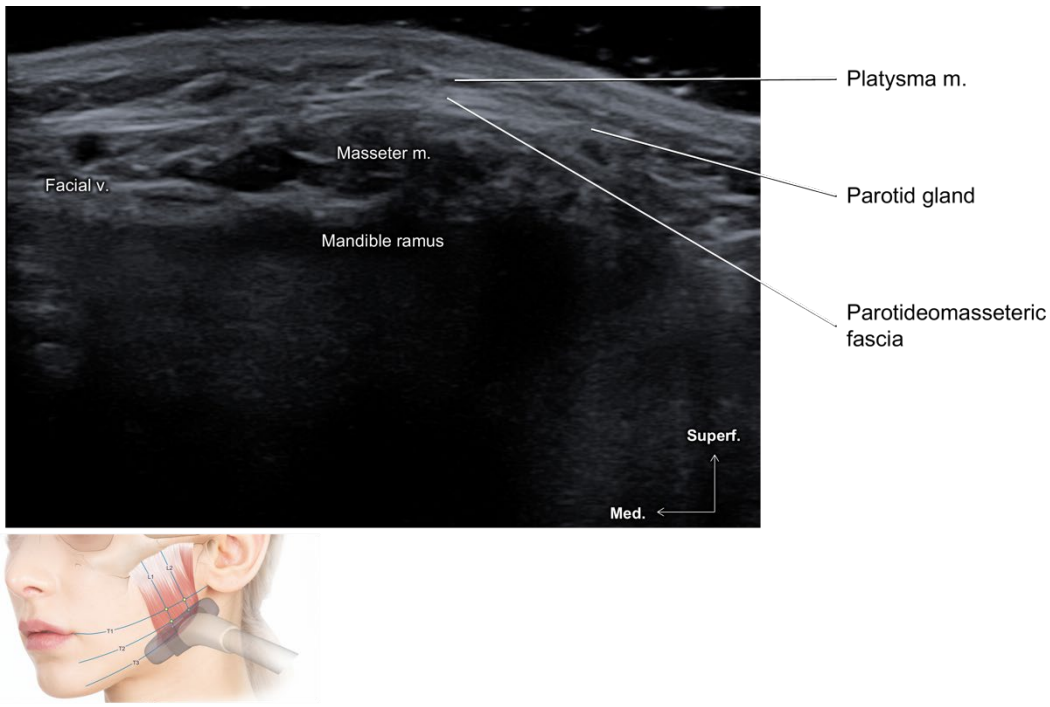

Figure 14. Ultrasonography of the transverse line corresponding to the lower margin of the mandible (T3), B mode (transverse view, 15 MHz by linear transducer)

Line L1

L1 is the anterior one-third line trisecting the masseter longitudinally. The skin and subcutaneous layer are observed most superficially as in other images. Mandibular ramus is observed as a strong hyperechoic line, and a hypoechoic masseter muscle is observed directly above it. Inside the muscle, hyperechoic DITs are observed. On the surface of the masseter, a platysma muscle shown as an irregular hypoechoic band is located, which is extended from the cervical area (Figure 15).

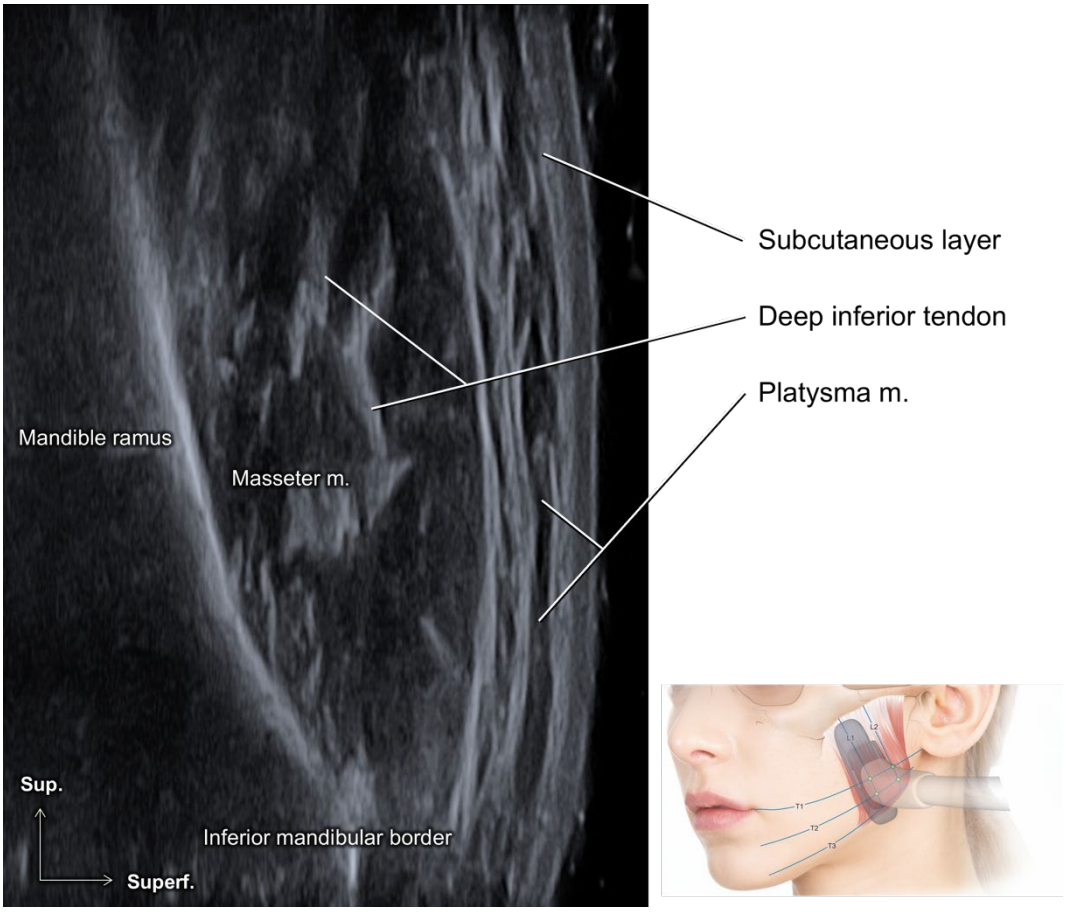

Figure 15. Ultrasonography of the anterior one-third line trisecting the masseter longitudinally (L1), B mode (transverse view, 15 MHz by linear transducer)

Line L2

L2 is the posterior one-third line trisecting the masseter longitudinally. The US image at this position shows a similar pattern as in L1. Since the line is located posterior to the L1, a uniform hyperechoic parotid gland located superficially than the masseter muscle is well observed. Hyperechoic parotideomasseteric fascia enclosing the surface of the masseter and parotid gland is observed (Figure 16).

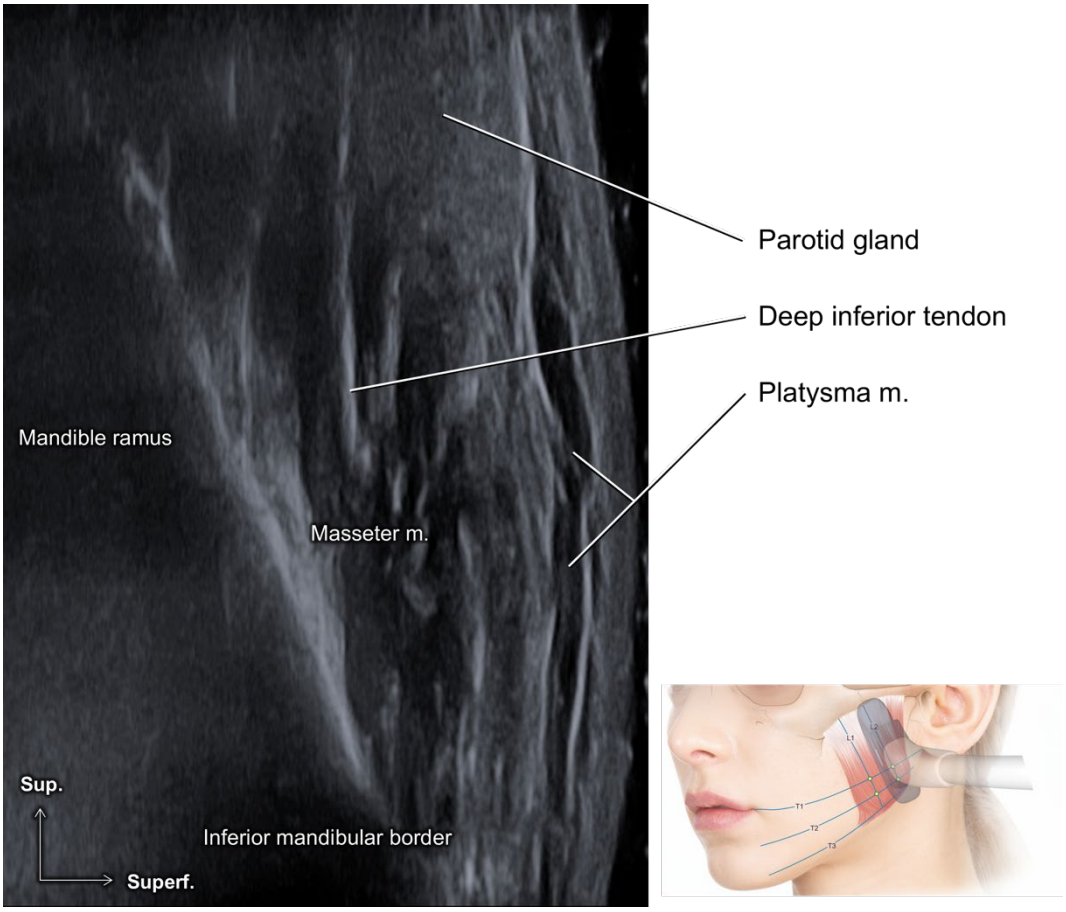

Figure 16. Ultrasonography of the posterior one-third line trisecting the masseter longitudinally (L2), B mode (transverse view, 15 MHz by linear transducer)

Normal US anatomy of the LPM area

The masseter, temporalis, and LPM were observed through the mandibular notch in all cases and located in order from the most superficial to the deepest (Figure 17). The mean thicknesses of the skin and subcutaneous layer, masseter muscle, and temporalis muscle, and depth of the LPM were 9.7±1.0 mm, 10.3±1.3 mm, 10.9±1.6 mm, and 30.9±1.9 mm, respectively at the MP (Figure 18).

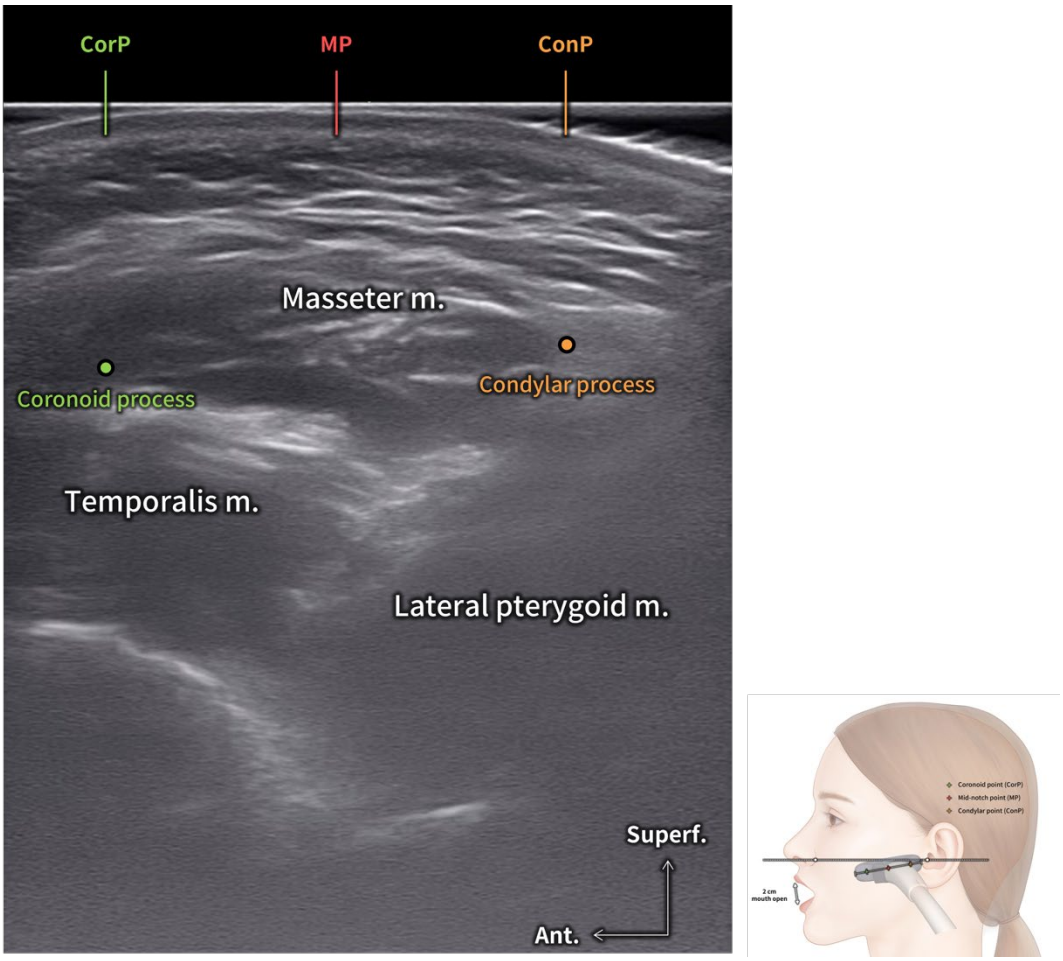

Figure 17. Ultrasonography of the lateral pterygoid muscle through the mandibular notch, B mode (transverse view, 15 MHz by linear transducer)

CorP, location of the coronoid process; ConP, location of the condylar process; MP, midpoint between CorP and ConP

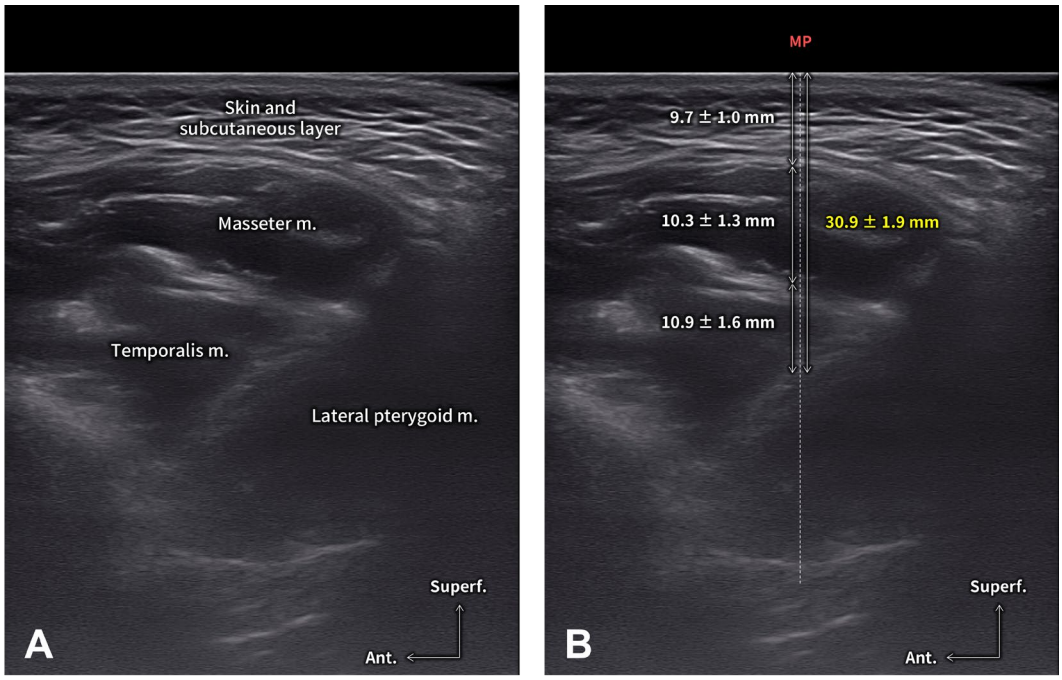

Figure 18. Ultrasonographic measurements at MP, B mode (transverse view, 15 MHz by linear transducer)

(A) Ultrasonography of the lateral pterygoid muscle through the mandibular notch (B) The mean thicknesses of the skin and subcutaneous layer, masseter muscle, temporalis muscle, and depth of the LPM were 9.7 ± 1.0, 10.3 ± 1.3 mm, 10.9 ± 1.6 mm, and 30.9 ± 1.9 mm, respectively at MP

CorP, location of the coronoid process; ConP, location of the condylar process; MP, midpoint between CorP and ConP

The location and the distribution of the CorP, MP, and ConP are listed in Table 1 and illustrated in Figure 19. The CorP was located 54.0±3.9 mm anterior to the tragus and 10.7±2.8 inferior to the ala-tragus line; the corresponding location for MP and ConP were 39.6±3.3 mm and 7.8±1.6, and 25.2±3.0 mm and 4.9±1.9 mm, respectively.

Table 1. Location of the reference points

Reference point	**x-axis**	**y-axis**
CorP		
Mean ± SD	54.0±3.9	10.7±2.8
Minimum	48.2	7.0
Maximum	61.7	15.1
MP		
Mean ± SD	39.6±3.3	7.8±1.6
Minimum	34.9	5.8
Maximum	46.2	10.6
ConP		
Mean ± SD	25.2±3.0	4.9±1.9
Minimum	21.6	0.7
Maximum	30.7	7.4

The data are expressed as mean±SD values (mm).

CorP, location of the coronoid process; ConP, location of the condylar process; MP, midpoint between CorP and ConP

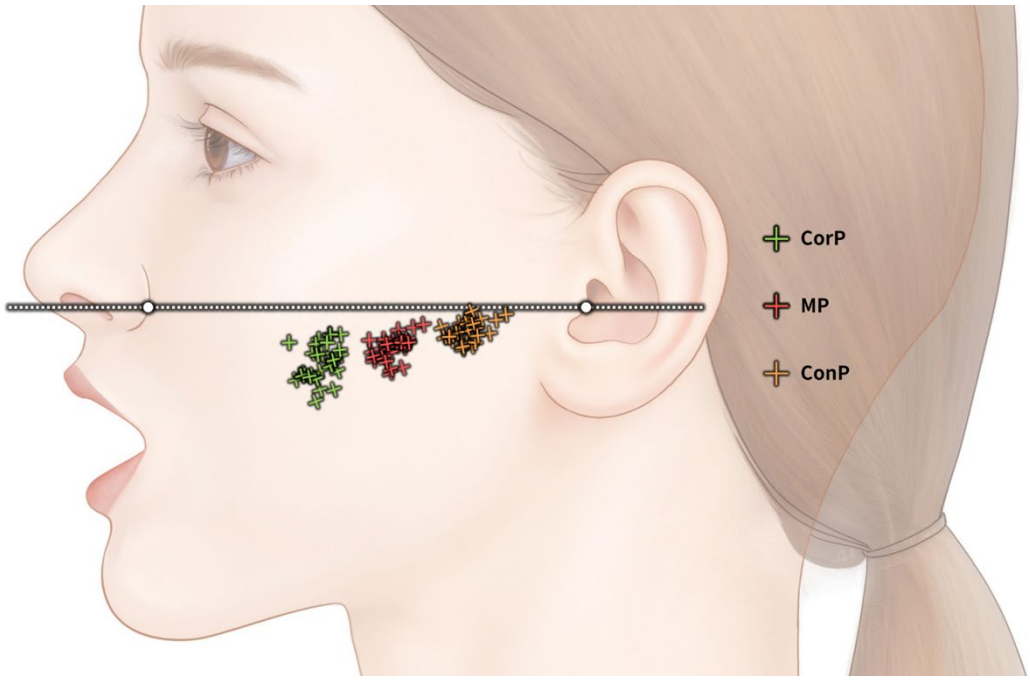

Figure 19. Distribution of the reference points relative to the ala-tragus line

CorP, location of the coronoid process; ConP, location of the condylar process; MP, midpoint between CorP and ConP

Part II: Comparison between the conventional blind injections and US-guided injections of botulinum toxin into the masseter

A case of PMB

One case of PMB was observed on the side where a conventional blind injection was administered. Soft bulging was evident in the anteroinferior area of the masseter while clenching at 3–4 days after the procedure (Figure 20). An immediate injection of 8 U of BoNT-A was administered to reduce the PMB. The superficial part of the masseter showed localized excessive contraction in the US image, which disappeared after the compensational injection, along with a reduction in PMB (Figure 21). There were no other side effects or complaints.

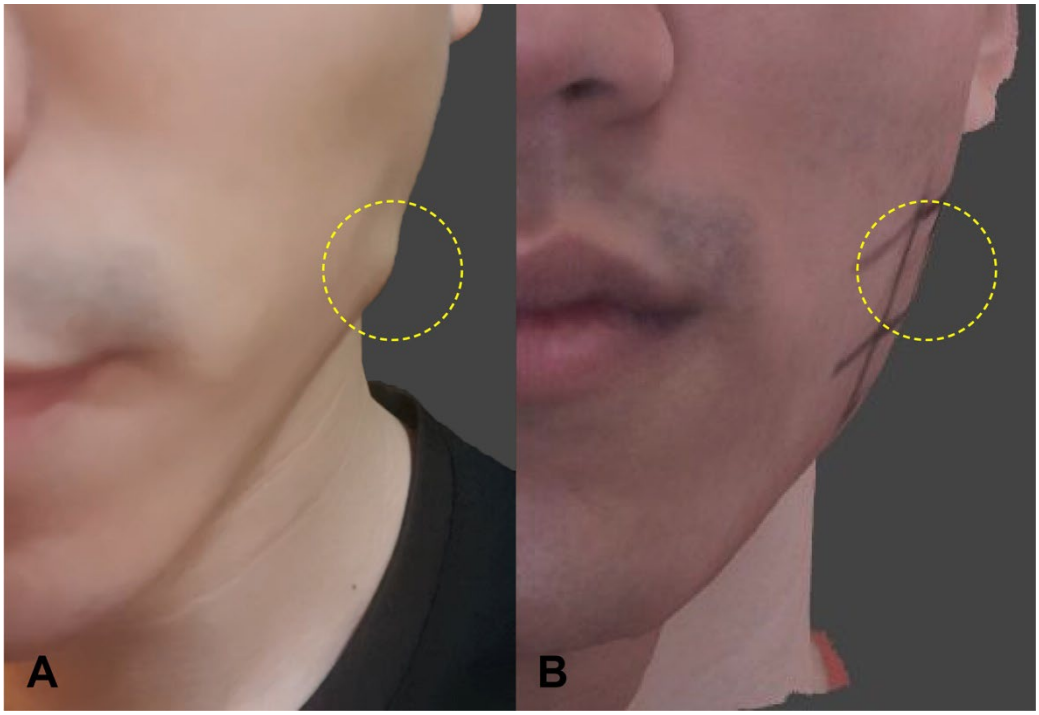

Figure 20. Photograph and 3D scanned models of paradoxical masseteric bulging (PMB) observed after a conventional blind injection

(A) Photograph showing soft bulging above the masseter while clenching (B) 3D scanned model showing that the PMB was reduced after making a compensational injection into an area that was more superficial than the deep inferior tendon.

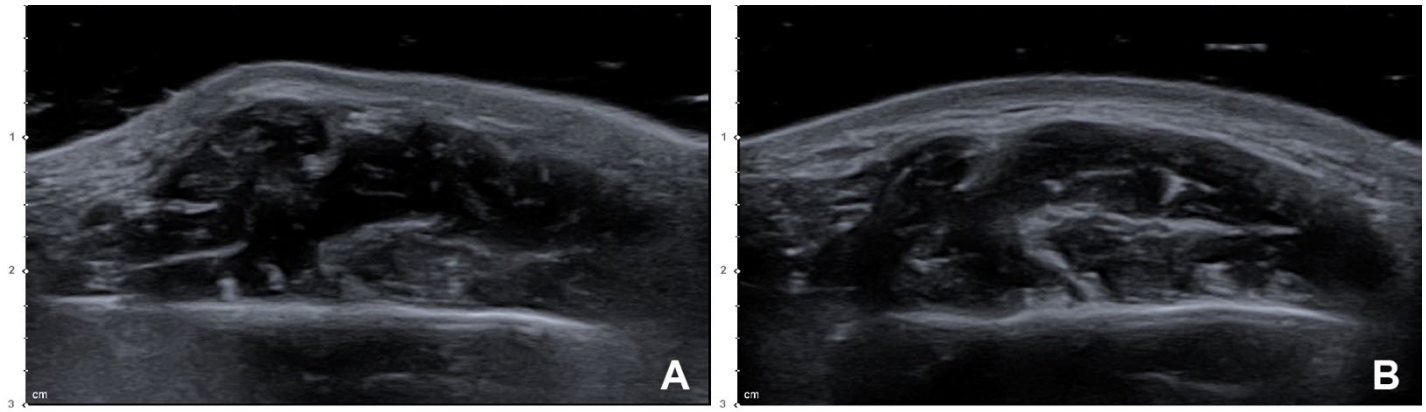

Figure 21. Ultrasonographic images of paradoxical masseteric bulging after performing the conventional blind injection

(A) Superficial part of the masseter showing localized excessive contraction while clenching (B mode, transverse view, 15-MHz linear transducer) (B) Localized excessive contraction in the clenching state that was resolved after performing a compensational injection of 8 U of botulinum toxin into the superficial part of the masseter (B mode, transverse view, 15-MHz linear transducer)

US-based analysis of the thickness of the masseter

The thicknesses of the masseters on the left and right sides were 12.3±2.9 mm (mean±SD) and 13.0±3.3 mm, respectively, before the injection, and 10.7±2.8 mm and 10.8±2.9 mm one month after the injection. The reduction in the thickness of the masseter in the resting state differed significantly at one month after the injection between the conventional blind injection group and the US-guided injection group (Figure 22) by 12.4±7.6% and 18.0±9.7%, respectively [$t(19)=3.059$, $p=0.007$] (Table 2).

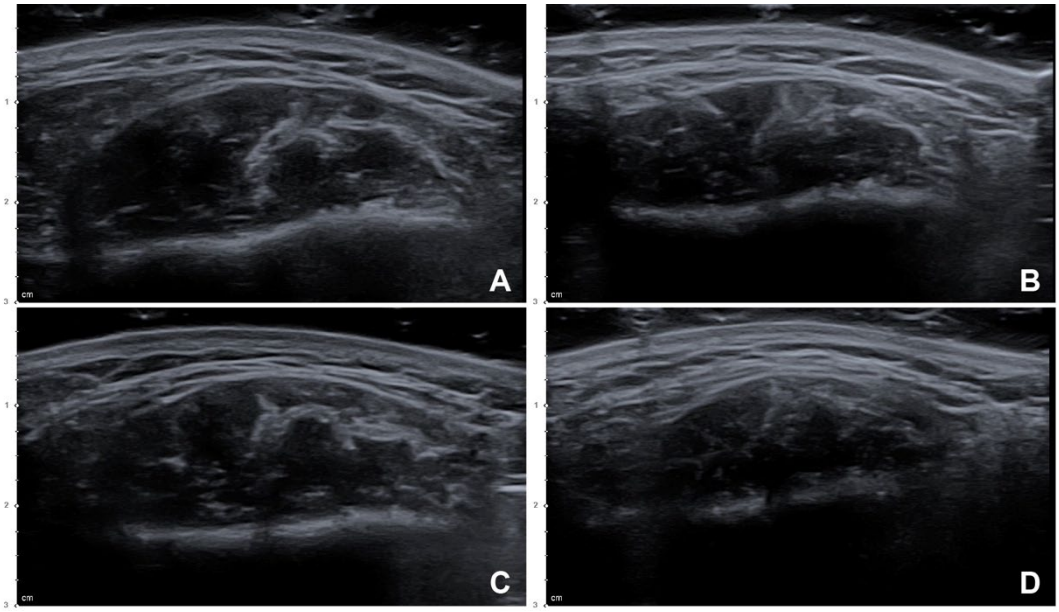

Figure 22. Ultrasonographic (US) images showing reduction of the masseter thickness after botulinum toxin injections, B mode, (transverse view, 15-MHz linear transducer)

(A) Left side, before the injection (B) Left side, one month after a conventional blind injection (C) Right side, before the injection (D) Right side, one month after a US-guided injection

Table 2. Measurements of differences in the masseter muscle thickness

Site	Injection method	Masseter thickness before injection (mm)	Masseter thickness at one month after the injection (mm)	Reduction in masseter thickness (%)	*p*
Left	Conventional blind injection (*n*=20)	12.3±2.9	10.7±2.8	12.4±7.6	0.007
Right	US-guided injection (*n*=20)	13.0±3.3	10.8±2.9	18.0±9.7	
Total	*n*=40	12.7±3.1	10.8±2.8	15.2±9.3	

Data are expressed as mean ± SD values.

Three-dimensional analysis of the facial contour

Most of the 20 volunteers (85%, n=17) showed a greater reduction in the facial contour on the US-guided injection side than on the blind injection side. The reduction in the facial contour was 2.0±0.7 mm in the conventional blind injection group and 2.2±0.8 mm in the US-guided injection group [t(19)=2.908, p=0.009] (Table 3).

Table 3. Measurements of the facial contour differences

Site	**Injection method**	**Depth difference between before and one month after the injection**	***p***
Left	Conventional blind injection (*n*=20)	–2.0±0.7 mm	0.009
Right	US-guided injection (*n*=20)	–2.2±0.8 mm	
Total	*n*=40	–2.1±0.8 mm	

Data are expressed as mean ± SD values.

Part III: Clinical anatomy of the DTAs

Topographic location of the DTAs

The measurements of the locations of the DTAs with reference to the VP are shown in Table 4 and Figure 23. The mean (range) distances between the VP, and the ADTA were 5.5 mm (2.1–9.7 mm), 4.6 mm (1.9–7.2 mm), and 2.5 mm (-5.0–14.6 mm) at H_{Za}, H_{Zt}, and H_{Eb}, respectively. The distances between the VP and the PDTA were 19.4 mm (13.2–24.6 mm), 21.7 mm (12.6–35.4 mm), and 25.3 mm (2.1–41.8 mm) at H_{Za}, H_{Zt}, and H_{Eb}, respectively. The locations of DTAs varied over a larger range at the level of the eyebrow (H_{Eb}) than at the lower levels (H_{Za} and H_{Zt}) (Figure 24). There were no significant differences between the Korean and Thai groups or between the male and female groups ($p > 0.05$).

Table 4. Distance between the deep temporal arteries (DTAs) and the vertical reference plane (VP) at each horizontal plane

DTA	H_{Za}	H_{Zt}	H_{Eb}
ADTA			
Mean±SD	5.5±2.2	4.6±1.7	2.5±6.5
Minimum	2.1	1.9	–5.0
Maximum	9.7	7.2	14.6
PDTA			
Mean±SD	19.4±3.1	21.7±5.3	25.3±10.3
Minimum	13.2	12.6	2.1
Maximum	24.6	35.4	41.8

N=22, unit: mm

SD, standard deviation

H_{Za}, horizontal plane through the zygomatic arch

H_{Zt}, horizontal plane through the zygomatic tubercle parallel to H_{Za}

H_{Eb}, horizontal plane through the eyebrow parallel to H_{Za}

ADTA, anterior deep temporal artery

PDTA, posterior deep temporal artery.

A negative value indicates that the arterial branch was located anterior to the VP

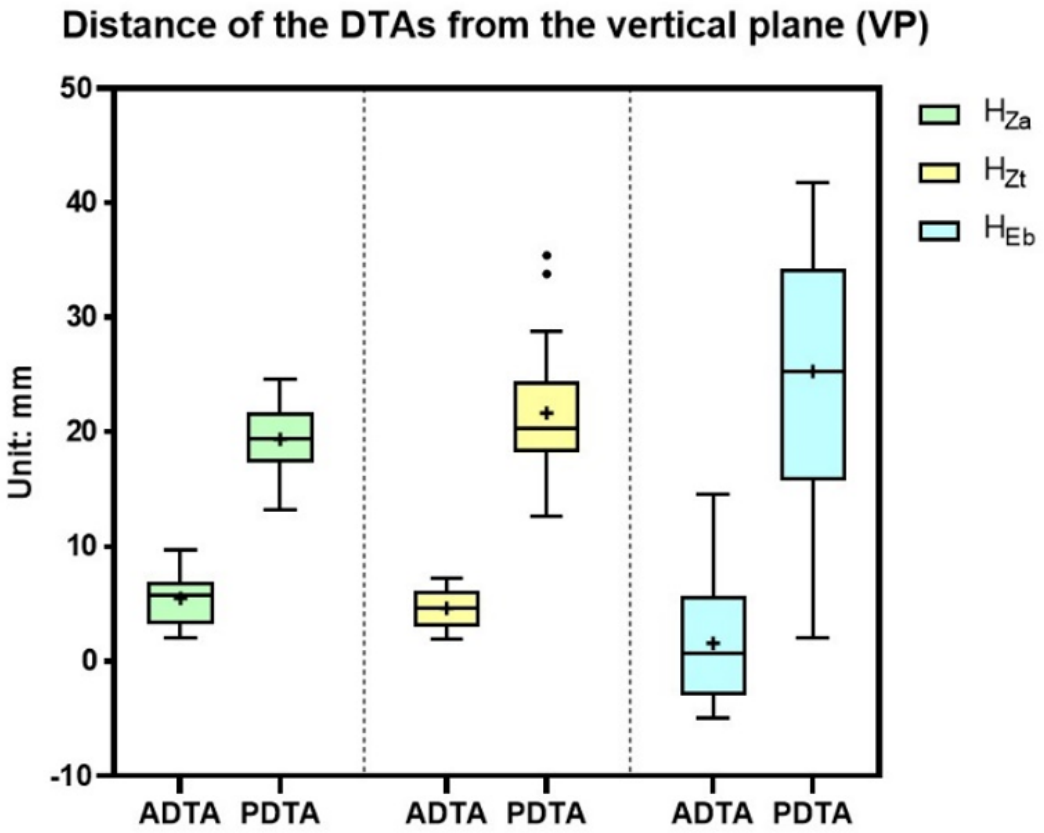

Figure 23. Distances of deep temporal arteries from the VP

DTAs, deep temporal arteries; VP, the vertical plane passing through the zygomatic tubercle perpendicular to the zygomatic arch; H_{Za}, the horizontal line passing through the zygomatic arch; H_{Zt}, the horizontal line passing through the zygomatic tubercle parallel to H_{Za}; H_{Eb}, the horizontal line passing through the eyebrow parallel to H_{Za}; ADTA, anterior deep temporal artery; PDTA, posterior deep temporal artery

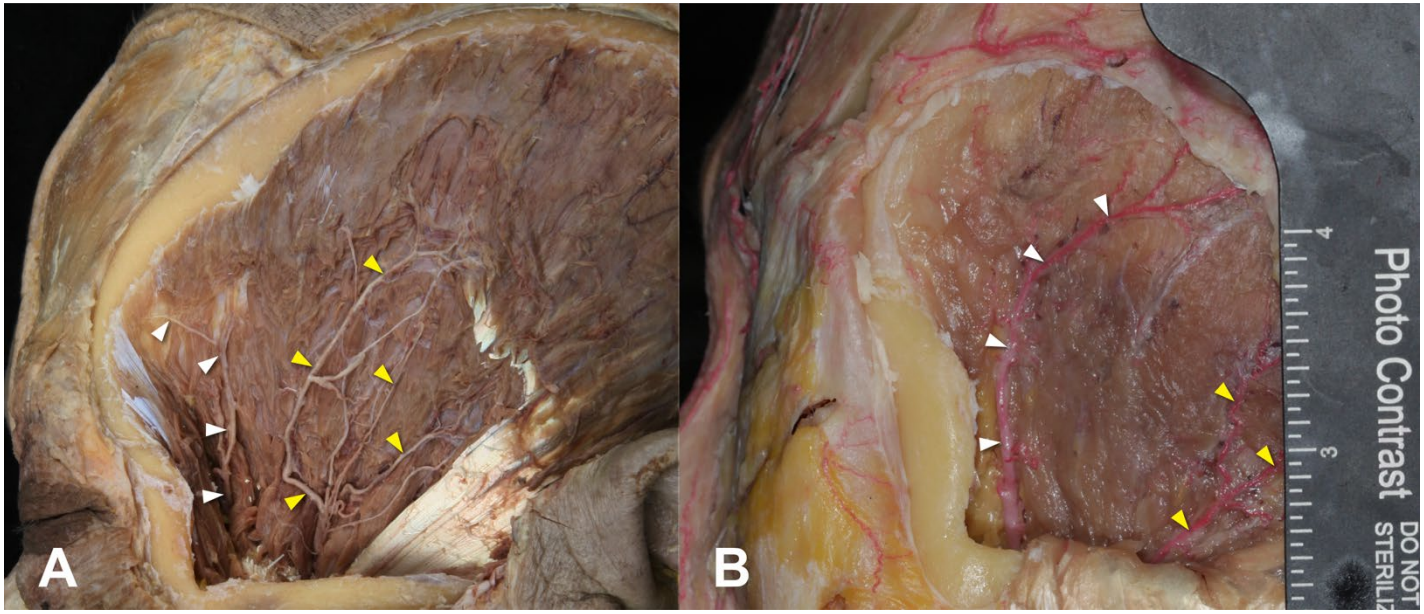

Figure 24. The courses of anterior deep temporal arteries (ADTA, white arrowheads) and posterior deep temporal arteries (PDTA, yellow arrowheads)

The courses of deep temporal arteries varied as they coursed superiorly in the temporalis muscle. The locations of the deep temporal arteries varied over a larger range at the level of the eyebrow than at the levels of the zygomatic arch and zygomatic tubercle. (A) Deep temporal arteries are located anteriorly (B) Deep temporal arteries are located posteriorly

Depth of the DTAs

The depths of DTAs were recorded based on measurements from the bony surface of the temporal fossa (Table 5 and Figure 25). The mean (range) distances between the bony surface of the temporal fossa, and the ADTA were 1.7 mm (0.3–5.5 mm) and 1.3 mm (0.2–3.1 mm) at H_{Zt} and H_{Eb}, respectively. The distances between the bone surface of the temporal fossa and the PDTA were 2.1 mm (0.4–4.6 mm) and 2.0 mm (0.1–5.2 mm) at H_{Zt} and H_{Eb}, respectively. There was no significant difference between the Korean and Thai groups or between the male and female groups ($p > 0.05$).

Table 5. Distance between the deep temporal arteries (DTAs) and the bony surface of the temporal fossa at each horizontal plane

DTA	H_{Zt}	H_{Eb}
ADTA		
Mean±SD	1.7±1.2	1.3±0.8
Minimum	0.3	0.2
Maximum	5.5	3.1
PDTA		
Mean±SD	2.1±1.2	2.0±1.4
Minimum	0.4	0.1
Maximum	4.6	5.2

N=58, unit: mm

SD, standard deviation

H_{Za}, horizontal plane through the zygomatic arch

H_{Zt}, horizontal plane through the zygomatic tubercle parallel to H_{Za}

H_{Eb}, horizontal plane through the eyebrow parallel to H_{Za}

ADTA, anterior deep temporal artery

PDTA, posterior deep temporal artery

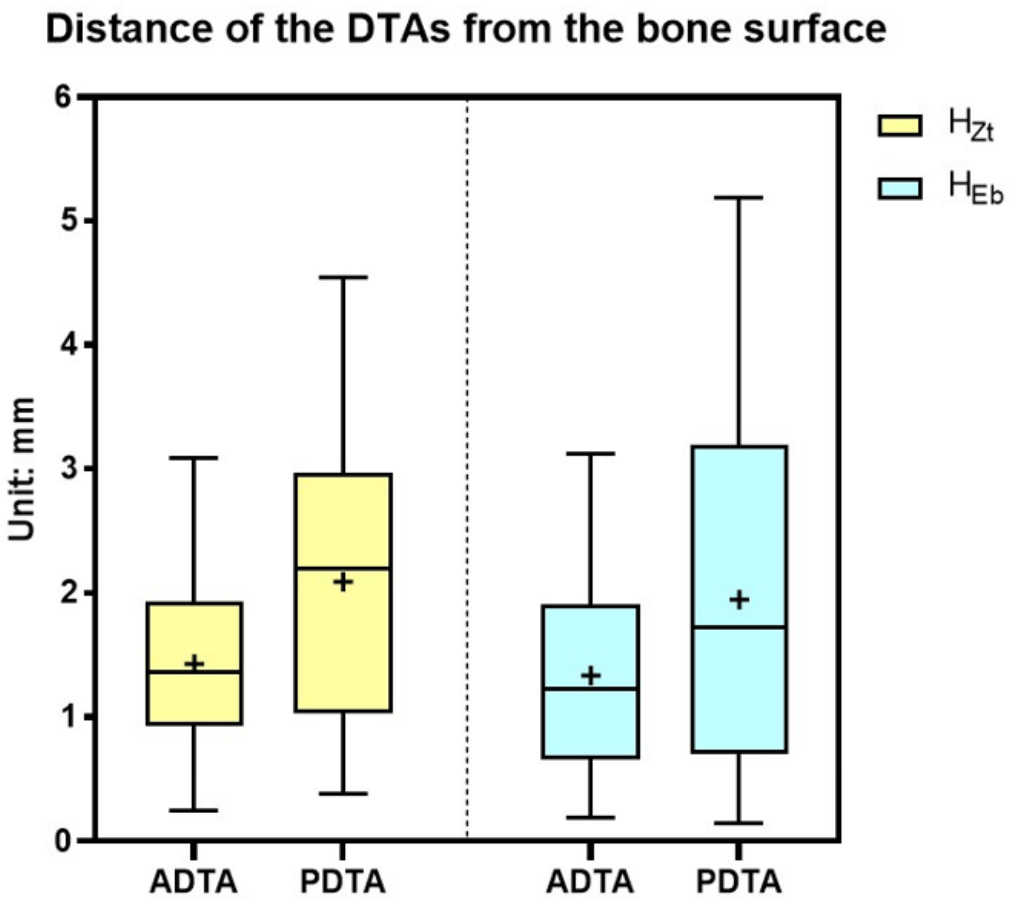

Figure 25. Distances of deep temporal arteries from the VP

DTAs, deep temporal arteries; VP, the vertical plane passing through the zygomatic tubercle perpendicular to the zygomatic arch; H_{Za}, the horizontal line passing through the zygomatic arch; H_{Zt}, the horizontal line passing through the zygomatic tubercle parallel to H_{Za}; H_{Eb}, the horizontal line passing through the eyebrow parallel to H_{Za}; ADTA, anterior deep temporal artery; PDTA, posterior deep temporal artery

IV. Discussions

Part I: Normal US anatomy of the masticatory muscles for the US-guided injection

US imaging has been widely used in various fields for both the diagnosis and treatment of disorders. It is easy to use and enables visualization of the internal structures in real-time with almost no harmful side effects. In contrast to other sites, the facial area has been rarely analyzed by US previously due to the presence of complex and multilayered anatomical structures. However, the increasing demand for minimally invasive esthetic procedures has resulted in clinicians beginning to utilize US technologies for guiding accurate injection procedures, and related studies have also been conducted (Lee et al., 2019; Choi et al., 2019).

A sound understanding of the three-dimensional anatomy of the masticatory muscles is important while performing various clinical procedures, such as minimally invasive and surgical procedures in the facial area. This study discussed the normal anatomy of the masticatory muscle and surrounding anatomical structures. A good anatomical understanding and the ability to interpret US images are essential for properly utilizing the US-guided injection technique.

The temple area is a multilayered structure that contains various important anatomical structures. From superficial to deep, the layers of the temporal fossa are arranged as follows: skin, subcutaneous tissue, STF, subSMAS layer, DTF, temporalis muscle, and periosteum layer. At least three distinct fatty components are also found in the temporal fossa: the subSMAS layer (between the STF and the superficial layer of the DTF), temporal fat pad (between the superficial and deep layers of the DTF above the zygomatic arch), and temporal extension of the buccal fat pad between the deep layer of the DTF and the temporalis muscle (Babakurban et al., 2010). Since the main anatomical structures to be considered during the procedure, including superficial temporal artery, middle temporal vein, facial nerve, and DTA, are located layer by layer, it is important to be able to distinguish these layered structures.

The masseter is one of the largest muscles in the facial area and can be easily identified by the naked eye and by palpation. Therefore, the injection into this muscle was considered to be simple. However, there are important anatomical structures present in this area, which are to be considered before the administration of injections. The origin of the risorius muscle generally covers the anterior third of the masseter on the SMAS layer. In addition, the thin platysma muscle, continued from the cervical area, covers the muscle and parotid gland. Therefore, injecting the toxin too anteriorly or shallowly can result in unintended paralysis of the risorius muscles, which can shorten the mouth or result in facial asymmetry while grinning (Bae et al., 2014). Deep injections to the bony surface also help clinicians prevent unintentionally injecting into the parotid gland, which usually

covers the posterior one-fourth of the masseter (Hu et al., 2010). Furthermore, the masseteric nerve is known to innervate the lower part of the muscle; therefore, injecting into the lower third of the masseter would maximize the effect of the toxin (Kim et al., 2010).

Several decades have passed since the botulinum toxin injection was first applied to the LPM for therapeutic purposes; it is not popularly implemented due to its deep and complex location. Several studies have tried to overcome these difficulties through the manufactured guide using CT and MRI (Yoshida, 2018; Pons et al., 2019). The proposed approach is largely divided into extraoral and intraoral approach. Among them, the extraoral approach uses a space formed by the zygomatic arch and mandibular notch as a "window" for the injection (Altaweel et al., 2019). In this study, the location of this space is presented in order to suggest an accurate guideline for an extraoral approach. The MP, which can be assumed as the midpoint of the mandibular notch space, was located 39.6±3.3 mm anterior and 7.8±1.6 mm inferior to the tragus.

US image obtained from this MP showed a constant appearance. Deep to the skin and subcutaneous layer, the masseter muscle was located most superiorly. The lateral surface of the coronoid process and condylar process were observed as hyperechoic short lines. At a deeper position, the temporalis muscle was located anteriorly and superficially, whereas the LPM was located posteriorly and deeply. The position of each structure can be confirmed once again by comparing them with the cross-sectional image of the head (Figure 26) (Park et al., 2005).

According to the measurement results, the distance from the skin to LPM at the MP was 30.9 ± 1.9 mm. Therefore, in order to access the LPM at this location, the injection should be performed at a depth of at least 3 cm. However, as can be seen from the US images, the LPM is not located parallel to the skin. This may vary depending on the morphology of the individual's facial contour, and the depth of the muscle may vary if the injection point is moved a little from the MP. Therefore, for clinical application, it is recommended to check the precise location of MP and LPM through the US analysis before the injection.

In addition to the LPM, the US image at this location shows the upper part of the masseter and the tendinous part of the temporalis. In indications that require an approach to these areas, the results of the present study will be helpful.

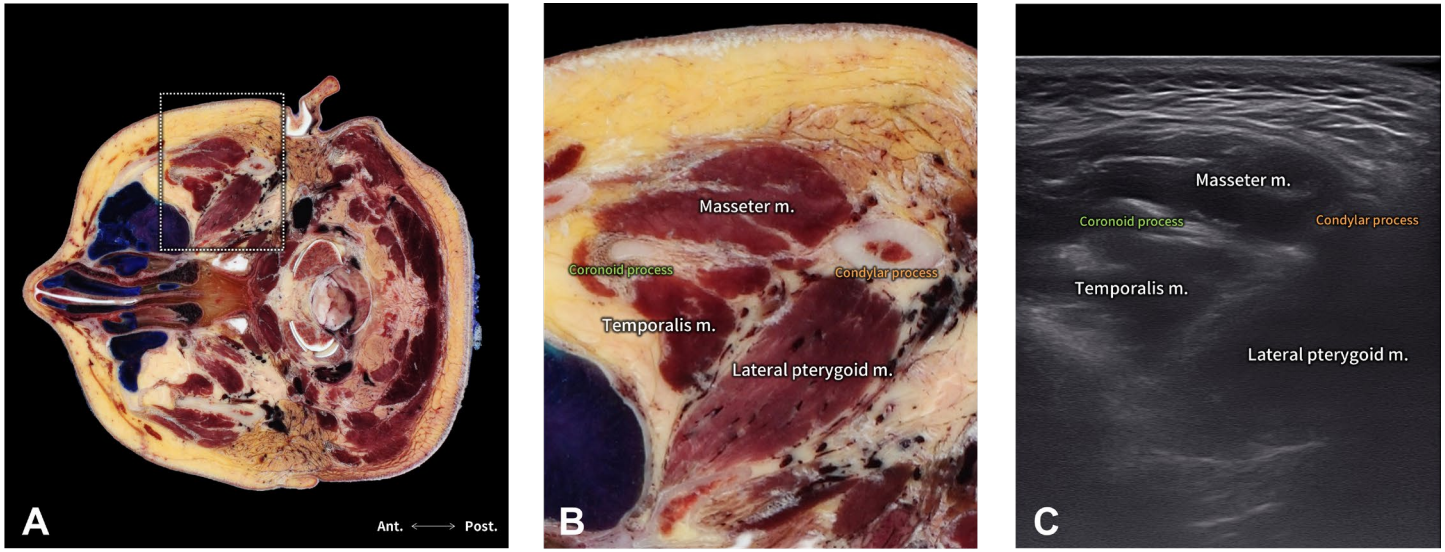

Figure 26. Comparison between cross-section image and ultrasonographic (US) image of lateral pterygoid muscle (A) Cross-section image of the head at the level of mandibular notch (B) Magnified cross-section image (C) US image obtained at the level of mandibular notch

*Cross-section was adapted from Visible Korean human co-produced by KISTI and Ajou University School of Medicine. “Park, J. S., Chung, M. S., Hwang, S. B., Lee, Y. S., Har, D. H., & Park, H. S. (2005). Visible Korean human: improved serially sectioned images of the entire body. IEEE transactions on medical imaging, 24(3), 352-360.”

Part II: Comparison between the conventional blind injections and US-guided injections of botulinum toxin into the masseter

According to the conventional guideline, the botulinum toxin should be injected deeply into three or four locations on the lower third of the masseter muscle, and this guideline is still commonly followed (Kim et al, 2016). This is a method of deep injection in which the needle tip contacts the bony surface of the mandible, and it minimizes the adverse effects on the surrounding anatomical structures previously mentioned.

While botulinum toxin injections are known to be relatively safe when the appropriate dose is used, there are still some adverse effects, such as the development of PMB, that are of concern to both clinicians and patients when using botulinum toxin to treat the masseter. The etiology of PMB is still unclear, but it is assumed that the deep part of the muscle is less affected when the toxin is injected deeply (Peng et al., 2018). It is known that individual differences in the contractions of the three layers of the masseter result in various types of bulging (Xie et al., 2014). It has also been reported that a strong DIT inside the masseter may prevent the spread of toxin, as well as individual differences in the morphology of the DIT (Lee et al., 2016; Lee et al., 2019). It can therefore be inferred that an imbalance of the contractile capability of the masseter induced by the deep injection method and the diffusion-inhibiting effect of DIT can cause PMB due to excessive contraction of the superficial layer. Although botulinum toxin is known to spread a few centimeters from the needle tip immediately after it is injected, a thick

muscle and diffusion restriction by the DIT can prevent the toxin from spreading across the muscle when using that conventional blind method in which the injection is administered just above the bony surface (Kinnett et al., 2004).

In order to minimize the probability of PMB occurrence, it is recommended to inject the botulinum toxin through the entire masseter while considering the DIT. A method of pulling back the needle after contacting the bony surface has been suggested to prevent the occurrence of PMB (Lee et al., 2016). However, in the actual blind injection procedure, clinicians cannot locate the DIT due to its morphological variations in individuals. Moreover, it has been reported that when a blind injection is performed in which the skin is premarked and injected percutaneously, the toxin is frequently injected too anteriorly (in up to 40% of cases) or the needle does not reach the desired depth due to its short length (up to 20% of cases) (Quezada-Gaon et al., 2016).

A US-guided injection can be utilized instead of a blind injection to locate the DIT accurately and to administer a precise injection. The real-time visualization of the intramuscular structures and needle location allows for accurate location of the targets. This also helps the clinician avoid structures that should not be affected, including facial expression muscles, blood vessels, and the parotid gland. US-guided injections have already been used to detect and target small structures, such as the risorius muscle (Lee et al., 2018). It is expected that if US-guided injections are used to inject into the multilayer masseter selectively, the muscle reduction will be more effective and PMB will be prevented.

The present study analyzed the changes in muscle thickness and overall facial contour at one month after the US-guided and conventional blind injections, which revealed a significant difference in the reduction of the masseter (17.98±7.59% and 12.38±9.65%, respectively; p=0.007) and in the facial contour change (–2.22±0.84 mm and –1.95±0.74 mm, p=0.009). These results suggest that, in contrast with the conventional method, a US-guided injection distributes the toxin across all regions, resulting in a volume reduction effect over the entire area. Reducing both the deep and superficial parts of the superficial layer in consideration of the DIT through a US-guided injection is not only meaningful for preventing PMB but also influences the amount of the volume reduction and facial contour changes. Regarding the adverse effects, one case of PMB occurred in the conventional blind injection group. This number is too small to statistically confirm that US-guided injection effectively reduces the incidence of PMB. Therefore, more cases need to be evaluated in future studies.

US-guided injections of the masseter have several advantages over conventional blind injections. First, this method allows the injection to be administered while considering the location of the DIT. Clinicians can prevent PMB by injecting into parts of the muscle that are both deeper and more superficial than the DIT. Furthermore, if necessary, a small-dose injection can be administered only at the desired location, depending on the bulging type. Second, US-guided injection makes it possible to identify the location of the masseter and surrounding structures in real-time before and during the procedure. The locations of the boundary of the masseter, the parotid gland on the posterior side of the

masseter, and the risorius and buccinator muscles on the anterior side of the masseter can be determined in order to protect these structures while injecting the botulinum toxin, as well as to ensure that the toxin is injected outside the muscle. Third, a larger volume reduction effect can be obtained with the same dose of toxin. In general, it is known that the toxin dose is not associated with the amount of volume reduction above a certain dose threshold. However, the results of the present study reveal that greater muscle thickness and facial contour reductions can be obtained through a US-guided injection.

A US-based evaluation provides much evidence about the anatomy of the masseter and the clinical application of botulinum toxin. In addition, this study has demonstrated that a US-guided injection method that considers the DIT by visualizing the masseter can prevent the occurrence of PMB during a blind injection and is more effective.

Part III: Clinical anatomy of the DTAs

A decrease in the soft-tissue component results in an aged appearance. Several materials have been utilized for soft tissue augmentation to compensate for this, including fat grafts, poly L-lactic acid, and hyaluronic acid (McNichols et al., 2012; Vrcek et al., 2015). Of these, hyaluronic acid is the most widely used material and is formulated with different levels of hardness and elasticity according to its suitability for different placement layers.

The rapidly increasing demand for temple augmentation has resulted in numerous proposals for temple augmentation techniques. Filler injections in the temple area are primarily administered using two methods: superficial and deep injections. Superficial temple injections target the layer between the STF and DTF. Several studies have suggested that this plane is safe for such injections because visible blood vessels can be easily avoided (Chundury et al., 2015; Lambros, 2011; Moradi et al., 2011).

Deep temple augmentation is performed at the supraperiosteal layer of the temporal fossa. This procedure is known to have the lowest risk of intravascular injection because there are only a few major blood vessels in this plane (Kim et al., 2016). Deep injections above the periosteal layer allow the clinicians to avoid three anatomical structures: the superficial temporal artery running within the STF, the middle temporal vein traveling along the intermediate fat pad, and the middle temporal artery that branches to provide blood supply to the deep surface of the posterior third of the temporalis muscle (Jung et

al., 2014; Talmage et al., 2015). Based on this anatomical knowledge, the supraperiosteal layer has also been suggested as a safe plane for injection.

Physicians have developed several techniques for deep temple augmentation. Raspaldo suggested that deep filler injection into the temple area should start with the anteroinferior quadrant to provide higher projection and greater volume and avoid facial nerve injury (Raspaldo, 2012). Other suggestions have also been based primarily on the following factors: effective volumization, the avoidance of the superficial temporal artery, and the notion that the arterial connection of DTAs is limited to the muscle (Juhász et al., 2015; Kim et al., 2016; Sykes et al., 2015). However, DTAs are known to anastomose with nearby vessels, such as the lacrimal and supraorbital arteries, and are important to consider when performing deep temple augmentation procedures (Quisling et al., 1975; Chen et al., 2014).

The present study confirmed that DTAs run through the layer targeted by deep temple augmentation procedure. The minimum distances between the bone and the DTA were less than 0.5 mm at the H_{Zt} and H_{Eb} levels. This implies that a deep temple augmentation procedure at any level might damage DTAs or lead to intravascular injection. Therefore, injection into the periosteal layer is not sufficient to avoid critical vascular complications, such as blindness or cerebral infarction. Moreover, as the depth of DTAs varies over a wide range within the temporalis muscle, there is no alternative safe plane available for deep injection procedures.

Based on our findings regarding vascular location and depth, we suggest only one safe site for deep temple augmentation procedures. No DTA branch was observed within 7.2–12.6 mm posterior to the zygomatic tubercle. Therefore, the area located 1 cm behind the VP at the level of the zygomatic tubercle (H_{Zt}) can be suggested as the safe site for the injection (Figure 27).

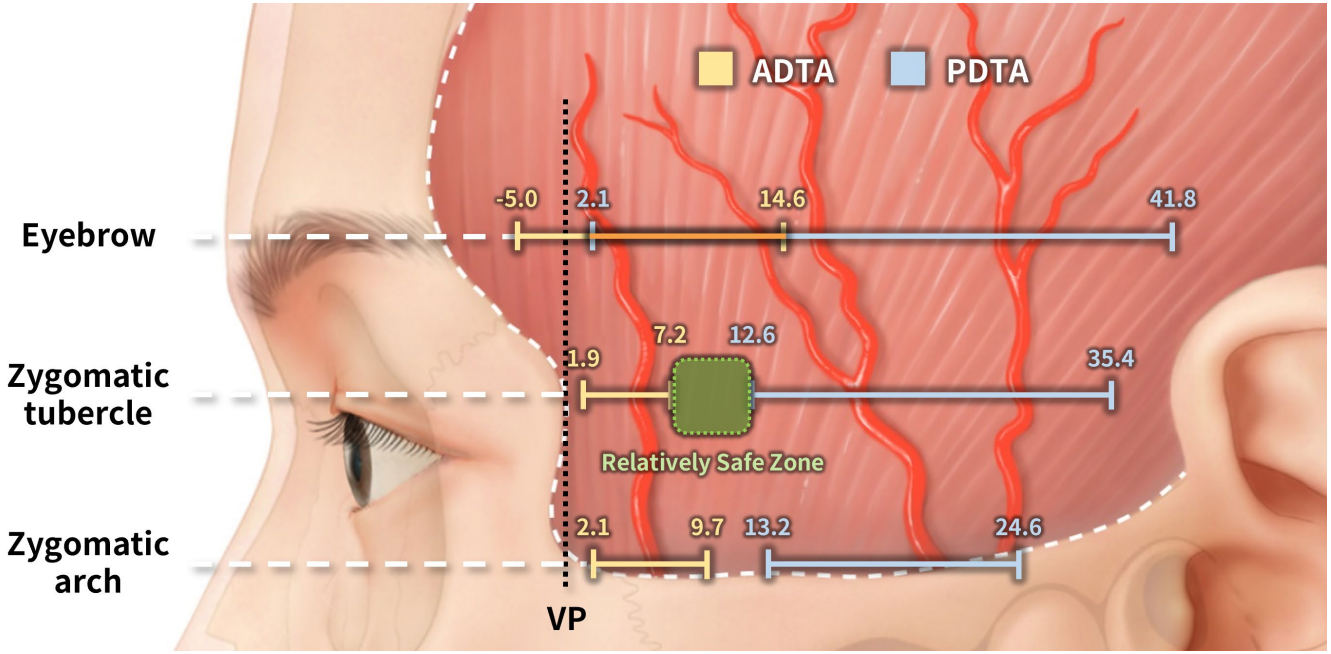

Figure 27. Schematic representation of the range of locations of the ADTA and the PDTA from the VP

The mean (range) distances between the VP and the ADTA are 5.5 mm (2.1–9.7 mm), 4.6 mm (1.9–7.2 mm), and 2.5 mm (-5.0–14.6 mm) at H_{Za}, H_{Zt}, and H_{Eb}, respectively. The distances between the VP and the PDTA are 19.4 mm (13.2–24.6 mm), 21.7 mm (12.6–35.4 mm), and 25.3 mm (2.1–41.8 mm) at H_{Za}, H_{Zt}, and H_{Eb}, respectively. Yellow, blue, and

orange shaded bars indicate areas where the ADTAs, PDTAs, and both ADTAs and PDTAs are located, respectively. At the level of the H_{Eb}, both DTAs can be located within the area that is 2.1–17.2 mm away from the VP.

ADTA, anterior deep temporal artery; PDTA, posterior deep temporal artery; VP, the vertical plane passing through the zygomatic tubercle perpendicular to the zygomatic arch; H_{Za}, the horizontal line passing through the zygomatic arch; H_{Zt}, the horizontal line passing through the zygomatic tubercle parallel to H_{Za}; H_{Eb}, the horizontal line passing through the eyebrow parallel to H_{Za};

In contrast, we did not find any safe area at the level of the eyebrow (H_{Eb}). Either DTA branch could be located within the wide range of 2.10–17.23 mm behind the VP. Moreover, at the H_{Eb} level, the distances from the bone to the ADTA and PDTA varied over the ranges of 0.20–1.57 and 0.39–4.51 mm, respectively. Since clinicians cannot detect the location and depth of DTAs without utilizing imaging methods (such as US), additional care is needed at the level of the eyebrow (H_{Eb}) to minimize the risks of a deep temple augmentation procedure.

US imaging helps visualize internal anatomical structures in real-time; therefore, it is actively used for diagnosis, research, and treatment of various disorders (Bae et al., 2020; Church et al., 2017; Ciftci et al., 2013; Kim et al., 2020). The Doppler mode can detect and visualize the frequency changes that occur when ultrasonic waves are reflected by flowing blood. The Doppler mode can detect not only the location of the blood vessel but also the movement direction and pulse of the blood; therefore, the operator can determine whether the blood vessel is an artery or a vein (Kim et al., 2020). Therefore, utilizing the Doppler mode to detect the positions of blood vessels in the temporal fossa is the optimal way to avoid intravascular injection while performing temple augmentation. To safely perform temple augmentation at the level of the eyebrow or above, clinicians should perform aspiration and reduce the risk by using slow infusion and small doses of injections. However, aspiration alone is insufficient because a high-viscosity and high-density filler may provide false-negative results. Moreover, deep temple augmentation requires a higher volume of filler than superficial temple augmentation to achieve the

same effect. Careful monitoring of patient responses and degradable filler materials will also help reduce serious risks.

V. Conclusion

This study provides detailed information on the clinical anatomy of the masticatory muscles and suggests the guidelines for US-guided minimally invasive procedures by 1) identifying the clinical anatomy of the masticatory muscles and surrounding structures through US, 2) comparing the conventional blind and the novel US-guided injection techniques in a clinical trial, and 3) clarify the anatomical features of DTAs through ultrasonographic and cadaveric analyses.

The conclusions of this study are as follows:

1. Precise location and morphology of the masticatory muscles and surrounding anatomical structures can be observed using US analysis.
2. The MP, which can be assumed to be the midpoint of the mandibular notch space, was 39.6±3.3 mm anterior and 7.8±1.6 mm inferior to the tragus. At this point, mean thicknesses of the skin and subcutaneous layer, masseter muscle, temporalis muscle, and the depth of the LPM were 9.7±1.0, 10.3±1.3 mm, 10.9±1.6 mm, and 30.9±1.9 mm, respectively.
3. Reducing both the deep and superficial parts of the superficial layer of the masseter muscle in consideration of the DIT through a US-guided injection is not only meaningful for preventing PMB but also showed a significant difference in the volume reduction and facial contour changes.

4. The area 1 cm posterior to the zygomatic tubercle may be used as a safe site for deep temple augmentation procedures. However, as the distribution patterns of the DTAs at H_{Eb} and depth of the DTAs are variable, additional care is required to minimize the risks of deep temple augmentation.

References

Ahn, J., Horn, C., & Blitzer, A. (2004). Botulinum toxin for masseter reduction in Asian patients. Archives of facial plastic surgery.

Altaweel, A. A., Elsayed, S. A. H., Baiomy, A. A. B. A., Abdelsadek, S. E., & Hyder, A. A. (2019). Extraoral versus intraoral botulinum toxin type A injection for management of temporomandibular joint disc displacement with reduction. Journal of Craniofacial Surgery, 30(7), 2149-2153.

Amans, M. R., Narvid, J., & Halbach, V. V. (2014). Intra-arterial chemotherapy for bilateral retinoblastoma via left ophthalmic artery and right anterior deep temporal artery. Case Reports, 2014, bcr2014204549.

Anugerah, A., Nguyen, K., & Nader, A. (2020). Technical considerations for approaches to the ultrasound-guided maxillary nerve block via the pterygopalatine fossa: a literature review. Regional Anesthesia & Pain Medicine, 45(4), 301-305.

Bae, H., Kim, J., Seo, K. K., Hu, K. S., Kim, S. T., & Kim, H. J. (2020). Comparison between conventional blind injections and ultrasound-guided injections of Botulinum toxin type A into the masseter: a clinical trial. Toxins, 12(9), 588.

Bae, J. H., Choi, D. Y., Lee, J. G., Seo, K. K., Tansatit, T., & Kim, H. J. (2014). The risorius muscle: anatomic considerations with reference to botulinum neurotoxin injection for masseteric hypertrophy. Dermatologic Surgery, 40(12), 1334-1339.

Beleznay, K., Carruthers, J. D., Humphrey, S., & Jones, D. (2015). Avoiding and treating blindness from fillers: a review of the world literature. Dermatologic Surgery, 41(10), 1097-1117.

Chen, Y. J., Chang, P. H., Chang, K. V., Wu, W. T., & Özçakar, L. (2018). Ultrasound guided injection for medial and lateral pterygoid muscles: a novel treatment for orofacial pain. Medical Ultrasonography, 20(1), 115-116.

Chen, Y., Wang, W., Li, J., Yu, Y., Li, L., & Lu, N. (2014). Fundus artery occlusion caused by cosmetic facial injections. Chinese medical journal, 127(08), 1434-1437.

Cheng, J., Hsu, S. H., & McGee, J. S. (2019). Botulinum toxin injections for masseter reduction in East Asians. Dermatologic Surgery, 45(4), 566-572.

Choi, Y. J., Lee, K. W., Gil, Y. C., Hu, K. S., & Kim, H. J. (2019). Ultrasonographic analyses of the forehead region for injectable treatments. Ultrasound in medicine & biology, 45(10), 2641-2648.

Chundury, R. V., Weber, A. C., McBride, J., Plesec, T. P., & Perry, J. D. (2015). Microanatomical location of hyaluronic acid gel following injection of the temporal hollows. Ophthalmic Plastic & Reconstructive Surgery, 31(5), 418-420.

Church, J. T., Gadepalli, S. K., Talishinsky, T., Teitelbaum, D. H., & Jarboe, M. D. (2017). Ultrasound-guided intrasphincteric botulinum toxin injection relieves obstructive defecation due to Hirschsprung's disease and internal anal sphincter achalasia. Journal of Pediatric Surgery, 52(1), 74-78.

Ciftci, T., Akinci, D., Yurttutan, N., & Akhan, O. (2013). US-guided botulinum toxin injection for excessive drooling in children.

Fujita, S., Iizuka, T., & Dauber, W. (2001). Variation of heads of lateral pterygoid muscle and morphology of articular disc of human temporomandibular joint–anatomical and histological analysis. Journal of oral rehabilitation, 28(6), 560-571.

Garcia, A., & Fulton Jr, J. E. (1996). Cosmetic denervation of the muscles of facial expression with botulinum toxin A dose-response study. Dermatologic surgery, 22(1), 39-43.

Guyuron, B., & Huddleston, S. W. (1994). Aesthetic indications for botulinum toxin injection. Plastic and reconstructive surgery, 93(5), 913-918.

Heylings, D. J., Nielsen, I. L., & McNeill, C. (1995). Lateral pterygoid muscle and the temporomandibular disc. Journal of orofacial pain, 9(1).

Horio, T., & Kawamura, Y. (1989). Effects of texture of food on chewing patterns in the human subject. Journal of oral rehabilitation, 16(2), 177-183.

Hu, K. S., Kim, S. T., Hur, M. S., Park, J. H., Song, W. C., Koh, K. S., & Kim, H. J. (2010). Topography of the masseter muscle in relation to treatment with botulinum toxin type A. Oral Surgery, Oral Medicine, Oral Pathology, Oral Radiology, and Endodontology, 110(2), 167-171.

Isola, G., Anastasi, G. P., Matarese, G., Williams, R. C., Cutroneo, G., Bracco, P., & Piancino, M. G. (2018). Functional and molecular outcomes of the human masticatory muscles. Oral Diseases, 24(8), 1428-1441.

Juhász, M. L. W., & Marmur, E. S. (2015). Temporal fossa defects: techniques for injecting hyaluronic acid filler and complications after hyaluronic acid filler injection. Journal of cosmetic dermatology, 14(3), 254-259.

Jung, W., Youn, K. H., Won, S. Y., Park, J. T., Hu, K. S., & Kim, H. J. (2014). Clinical implications of the middle temporal vein with regard to temporal fossa augmentation. Dermatologic Surgery, 40(6), 618-623.

Juniper, R. P. (1984). Temporomandibular joint dysfunction: a theory based upon electromyographic studies of the lateral pterygoid muscle. British Journal of Oral and Maxillofacial Surgery, 22(1), 1-8.

Kim, D. H., Hong, H. S., Won, S. Y., Kim, H. J., Hu, K. S., Choi, J. H., & Kim, H. J. (2010). Intramuscular nerve distribution of the masseter muscle as a basis for botulinum toxin injection. Journal of Craniofacial Surgery, 21(2), 588-591.

Kim, H. J., Seo, K. K., Lee, H. K., & Kim, J. (2016). Clinical anatomy for botulinum toxin injection. In Clinical Anatomy of the Face for Filler and Botulinum Toxin Injection (pp. 55-92). Springer, Singapore.

Kim, H. J., Youn, K. H., Kim, J. S., Kim, Y. S., Hong, S. O., & Na, J. (2020). Ultrasonographic Anatomy of the Face and Neck for Minimally Invasive Procedures: An Anatomic Guideline for Ultrasonographic-Guided Procedures. Springer Nature.

Kim, N. H., Chung, J. H., Park, R. H., & Park, J. B. (2005). The use of botulinum toxin type A in aesthetic mandibular contouring. Plastic and reconstructive surgery, 115(3), 919-930.

Kinnett, D. (2004). Botulinum toxin A injections in children: technique and dosing issues. American journal of physical medicine & rehabilitation, 83(10), S59-S64.

Lambros, V. (2011). A technique for filling the temples with highly diluted hyaluronic acid: the "dilution solution". Aesthetic Surgery Journal, 31(1), 89-94.

Lee, H. J., Choi, Y. J., Lee, K. W., Hu, K. S., Kim, S. T., & Kim, H. J. (2019). Ultrasonography of the internal architecture of the superficial part of the masseter muscle in vivo. Clinical Anatomy, 32(3), 446-452.

Lee, H. J., Kang, I. W., Seo, K. K., Choi, Y. J., Kim, S. T., Hu, K. S., & Kim, H. J. (2016). The anatomical basis of paradoxical masseteric bulging after botulinum neurotoxin type A injection. Toxins, 9(1), 14.

Lee, H. J., Kim, J. S., Youn, K. H., Lee, J., & Kim, H. J. (2018). Ultrasound-guided botulinum neurotoxin type A injection for correcting asymmetrical smiles. Aesthetic Surgery Journal, 38(9), NP130-NP134.

Lee, S. J., McCall Jr, W. D., Kim, Y. K., Chung, S. C., & Chung, J. W. (2010). Effect of botulinum toxin injection on nocturnal bruxism: a randomized controlled trial. American journal of physical medicine & rehabilitation, 89(1), 16-23.

Levy, L. L., & Emer, J. J. (2012). Complications of minimally invasive cosmetic procedures: prevention and management. Journal of cutaneous and aesthetic surgery, 5(2), 121.

McNichols, C. H., Hatef, D. A., Cole, P., Hollier Jr, L. H., & Thornton, J. F. (2012). Contemporary techniques for the correction of temporal hollowing: augmentation temporoplasty with the classic dermal fat graft. Journal of Craniofacial Surgery, 23(3), e234-e238.

Moradi, A., Shirazi, A., & Perez, V. (2011). A guide to temporal fossa augmentation with small gel particle hyaluronic acid dermal filler. Journal of Drugs in Dermatology: JDD, 10(6), 673-676.

Murray, G. M., Bhutada, M., Peck, C. C., Phanachet, I., Sae-Lee, D., & Whittle, T. (2007). The human lateral pterygoid muscle. Archives of Oral Biology, 52(4), 377-380.

Murray, G. M., Phanachet, I., Uchida, S., & Whittle, T. (2004). The human lateral pterygoid muscle: a review of some experimental aspects and possible clinical relevance. Australian dental journal, 49(1), 2-8.

Nakajima, H., Imanishi, N., & Minabe, T. (1995). The arterial anatomy of the temporal region and the vascular basis of various temporal flaps. British journal of plastic surgery, 48(7), 439-450.

Park, J. S., Chung, M. S., Hwang, S. B., Lee, Y. S., Har, D. H., & Park, H. S. (2005). Visible Korean human: improved serially sectioned images of the entire body. IEEE transactions on medical imaging, 24(3), 352-360.

Peng, H. L. P., & Peng, J. H. (2018). Complications of botulinum toxin injection for masseter hypertrophy: Incidence rate from 2036 treatments and summary of causes and preventions. Journal of cosmetic dermatology, 17(1), 33-38.

Peterson, L. J., & Naidoo, L. C. D. (1996). Lateral pterygoid muscle and its relationship to the meniscus of the temporomandibular joint. Oral Surgery, Oral Medicine, Oral Pathology, Oral Radiology, and Endodontology, 82(1), 4-9.

Pinar, Y. A., & Govsa, F. (2006). Anatomy of the superficial temporal artery and its branches: its importance for surgery. Surgical and Radiologic Anatomy, 28(3), 248-253.

Pons, M., Meyer, C., Euvrard, E., Weber, E., Sigaux, N., & Louvrier, A. (2019). MR-guided navigation for botulinum toxin injection in the lateral pterygoid muscle. First results in the treatment of temporomandibular joint disorders. Journal of Stomatology, Oral and Maxillofacial Surgery, 120(3), 188-195.

Qin, X., & Xie, X. (2020). Ultrasound-guided maxillary nerve block via the pterygopalatine fossa: maxillary artery is the key. Regional anesthesia and pain medicine, 45(12), 1028-1029.

Quezada-Gaon, N., Wortsman, X., Penaloza, O., & Carrasco, J. E. (2016). Comparison of clinical marking and ultrasound-guided injection of Botulinum type A toxin into the

masseter muscles for treating bruxism and its cosmetic effects. Journal of cosmetic dermatology, 15(3), 238-244.

Quisling, R. G., & Seeger, J. F. (1975). Orbital anastomoses of the anterior deep temporal artery. Neuroradiology, 8(5), 259-262.

Raspaldo, H. (2012). Temporal rejuvenation with fillers: global faceculpture approach. Dermatologic surgery, 38(2), 261.

Ruiz Santiago, F., Prados Olleta, N., Tomás Muñoz, P., Guzmán Álvarez, L., & Martínez Martínez, A. (2019). Short term comparison between blind and ultrasound guided injection in morton neuroma. European Radiology, 29(2), 620-627.

Standring, S., Ellis, H., Healy, J., Johnson, D., Williams, A., Collins, P., & Wigley, C. (2005). Gray's anatomy: the anatomical basis of clinical practice. American journal of neuroradiology, 26(10), 2703.

Statistics, P. S. P. (2021). American Society of Plastic Surgeons, 2020.

Sykes, J. M., Cotofana, S., Trevidic, P., Solish, N., Carruthers, J., Carruthers, A., ... & Remington, B. K. (2015). Upper face: clinical anatomy and regional approaches with injectable fillers. Plastic and reconstructive surgery, 136(5), 204S-218S.

Talmage, G. D., Sunde, J., Walker, D. D., Atlas, M. D., & Gluth, M. B. (2016). Anatomic basis of the middle temporal artery periosteal rotational flap in otologic surgery. The Laryngoscope, 126(6), 1426-1432.

Thanasarnaksorn, W., Cotofana, S., Rudolph, C., Kraisak, P., Chanasumon, N., & Suwanchinda, A. (2018). Severe vision loss caused by cosmetic filler augmentation: case series with review of cause and therapy. Journal of Cosmetic Dermatology, 17(5), 712-718.

To, E. W., Ho, W. S., Wong, W. K., Pang, P. C., Ahuja, A. T., Hui, A. C., & King, W. W. (2001). A prospective study of the effect of botulinum toxin A on masseteric muscle hypertrophy with ultrasonographic and electromyographic measurement. British journal of plastic surgery, 54(3), 197-200.

von Coelln, R., Raible, A., Gasser, T., & Asmus, F. (2008). Ultrasound-guided injection of the iliopsoas muscle with botulinum toxin in camptocormia. Movement disorders, 23(6), 889-892.

Vrcek, I., El-Sawy, T., Chou, E., Allen, T., & Nakra, T. (2017). Neuropathic pain following poly-L-lactic acid (Sculptra) injection. Ophthalmic Plastic and Reconstructive Surgery, 33(3), S11-S12.

Wongwatana, S., Kronman, J. H., Clark, R. E., Kabani, S., & Mehta, N. (1994). Anatomic basis for disk displacement in temporomandibular joint (TMJ) dysfunction. American Journal of Orthodontics and Dentofacial Orthopedics, 105(3), 257-264.

Wu, W. T. (2010). Botox facial slimming/facial sculpting: the role of botulinum toxin-A in the treatment of hypertrophic masseteric muscle and parotid enlargement to narrow the lower facial width. Facial Plastic Surgery Clinics, 18(1), 133-140.

Yeh, Y. T., Peng, J. H., & Peng, H. L. P. (2018). Literature review of the adverse events associated with botulinum toxin injection for the masseter muscle hypertrophy. Journal of cosmetic dermatology, 17(5), 675-687.

Yoshida, K. (2018). Computer-Aided Design/Computer-Assisted Manufacture--Derived Needle Guide for Injection of Botulinum Toxin into the Lateral Pterygoid Muscle in Patients with Oromandibular Dystonia. Journal of Oral & Facial Pain & Headache, 32(2).

Abstract (in Korean)

최소침습적 초음파 유도 시술을 위한 씹기근육의 임상 해부학

<지도교수 김희진>

연세대학교 대학원 치의학과

배 형 규

씹기근육(Masticatory muscle)은 다양한 얼굴 부위의 최소침습적 시술의 목표 부위가 된다. 씹기근육 내의 최소침습적 시술은 깨물근 내 보툴리눔 독소 주사 부위가 국한되어 나타나는 국소적 활성 정도 불균형으로 인한 보상성비대(paradoxical masseteric bulging), 관자근 내 혈관 속에 필러가 주입되어 나타나는 혈관 폐색과 이로 인한 실명, 뇌경색 등 여러 부작용을 초래할 수 있다. 이를 방지하기 위해서는 씹기근육에 대한 해부학적인 이해가 필수적이다.

초음파 진단법은 실시간으로 해부학적 구조의 동적인 변화를 관찰할 수 있고, 대상구조와 인접한 해부학적 구조물을 직관적으로 이해할 수 있는 장점이 있다. 이에 따라 시술 중 해부학적 구조와 주사점의 위치를 확인할 수 있는 최소침습적

초음파유도 시술의 활용 가능성이 대두되고 있고, 씹기근육에의 최소침습적 시술을 안전하게 시행할 수 있는 새로운 방법이 될 수 있을 것으로 기대된다.

이에 본 연구에서는 1) 초음파 측정을 통한 씹기근육과 주위 구조의 해부학적 정보를 구명하고, 2) 깨물근에 대한 보툴리눔 독소 주사의 초음파 유도 주사법과 기존의 암맹 주사법(blind injection)을 비교하고, 3) 관자근 내 깊은관자동맥(deep temporal artery)의 주행과 3 차원적 위치정보를 밝혀내어 씹기근육을 대상으로 한 최소침습적 시술의 안전한 가이드라인을 제시하고자 한다.

본 연구는 파트 I: 씹기근육의 초음파 정상해부학, 파트 II: 깨물근에 대한 보툴리눔독소 주사의 초음파유도주사법과 암맹주사법의 비교, 그리고 파트 III: 깊은관자동맥의 임상해부학으로 이루어졌다. 파트 I 에서는 총 80 명의 피험자의 160 쪽의 반쪽얼굴을 대상으로 깨물근, 관자근과 턱뼈패임을 통한 씹기근육과 그 주변 구조물의 정상해부학에 대한 분석을 진행하였다. 가쪽날개근과 그 주위 구조는 턱뼈패임과 광대활로 이루어진 공간을 통해서 관찰되기 때문에, 근육돌기(CorP), 관절돌기(ConP), 그리고 그 중간점(MP)의 위치를 기록하고 측정하였다. 또한 MP 에서 관찰되는 각 구조들과 가쪽날개근의 깊이를 측정하였다. 파트 II 에서는 20 명의 대상자의 깨물근을 대상으로 왼쪽과 오른쪽에 각각 암맹주사법과 초음파유도 주사법으로 24U 의 보툴리눔 독소(BoNT-A)를 주사하고, 주사 전과 직후, 한 달 후 근육의 두께와 얼굴 윤곽의 변화에 대해 초음파기기와 3D 스캐너를 통해 분석하였다. 파트 III 에서는 깊은관자동맥의 주행을 확인하기 위해

15 구의 한국 시신과 6 구의 태국 시신으로부터 42 쪽의 반쪽머리를 해부하였다. 또한 초음파의 도플러모드를 사용하여 깊은관자동맥의 관자부위의 뼈 표면으로부터의 거리를 측정하였다.

파트 I 에서, 관자근과 깨물근, 가쪽날개근과 그 주위 구조들을 초음파를 통해 분석하였다. 입을 2 cm 벌린 상태에서 턱뼈패임부위를 초음파로 분석한 결과 모든 경우에서 깨물근, 관자근, 가쪽날개근이 얕은 곳에서 깊은 곳 순서로 관찰되었다 (n=120). MP 에서 측정한 피부와 피부밑조직의 두께, 깨물근의 두께, 관자근의 두께, 피부로부터 가쪽날개근까지의 거리는 각각 9.7±1.0 mm, 10.3±1.3 mm, 10.9±1.6 mm, 30.9±1.9 mm 로 나타났다. 입을 2 cm 벌린 상태에서 CorP, MP, ConP 의 위치는 귀구슬에서 각각 54.0±3.9 mm, 39.6±3.3 mm, 25.2±3.0 mm 앞쪽, 10.7±2.8 mm, 7.8±1.6 mm, 4.9±1.9 mm 아래쪽에 위치하였다.

파트 II 에서 암맹주사법과 초음파유도 주사법의 비교 결과, 깨물근보상성비대가 암맹주사법 실험군에서 한 사례 발생하였다. 종속표본 t 검증 결과, 주사 한달 후 깨물근의 두께 감소량은 각각 12.4±7.8%와 18.0±9.7%로 유의한 차이를 보였다 ($p = 0.007$). 깨물근 풍융 부위의 윤곽 감소 또한 각각 2.0±0.7 mm, 2.2±0.8 mm 로 유의한 차이를 보였다 ($p=0.009$).

파트 III 에서 깊은관자동맥의 경우 광대결절(zygomatic tubercle)로부터 뒤쪽 7.2-12.6 mm 내에는 주행하지 않았으나, 눈썹 높이에서는 모든 범위에 분포하였다. 앞깊은관자동맥과 뼈 표면과의 거리는 광대결절과 눈썹 높이에서 각각 1.3±0.8

mm, 1.7±1.2 mm 로 나타났으며 뒤깊은관자동맥의 경우는 2.0±1.4 mm, 2.1±1.2 mm 로 나타났다.

본 연구에서는 위의 결과들의 바탕으로, 각 씹기근육의 초음파유도 주사법에 있어 필요한 정상해부학적 구조를 구명함과 더불어 효율적이고 안전한 초음파유도 최소침습적 시술에 대한 가이드라인을 제시하였다.

핵심 되는 말 : 초음파, 최소침습적 시술, 씹기근육, 보툴리눔독소, 필러주사, 깨물근, 관자근, 가쪽날개근